#036

SOURCE TARGET & LIST, TIME & RA ORDER

77-075A-02G

EXTRAGALACTIC X-RAY SOURCE CATALOG

77-075A-02E

77-075A-02D

HEAO 1

Table of Contents

----

1. INTRODUCTION:

The documentation for this data set was originally on paper, kept in NSSDC's Data Set Catalogs (DSCs). The paper documentation in the Data Set Catalogs have been made into digital images, and then collected into a single PDF file for each Data Set Catalog. The inventory information in these DSCs is current as of July 1, 2004. This inventory information is now no longer maintained in the DSCs, but is now managed in the inventory part of the NSSDC information system. The information existing in the DSCs is now not needed for locating the data files, but we did not remove that inventory information.

The offline tape datasets have now been migrated from the original magnetic tape to Archival Information Packages (AIP's).

A prior restoration may have been done on data sets, if a requestor of this data set has questions; they should send an inquiry to the request office to see if additional information exists.

2. ERRATA/CHANGE LOG:

NOTE: Changes are made in a text box, and will show up that way when displayed on screen with a PDF reader.

When printing, special settings may be required to make the text box appear on the printed output.

Version	Date	Person	Page	Description of Change
01				
02				

3 LINKS TO RELEVANT INFORMATION IN THE ONLINE NSSDC INFORMATION SYSTEM:

http://nssdc.gsfc.nasa.gov/nmc/

[NOTE: This link will take you to the main page of the NSSDC Master Catalog. There you will be able to perform searches to find additional information]

4. CATALOG MATERIALS:

a. Associated Documents — To find associated documents you will need to know the document ID number and then click here.
http://nssdcftp.gsfc.nasa.gov/miscellaneous/documents/

b. Core Catalog Materials

HEAD 1

NEW HARD X-RAY SOURCES

77-075A-02D

THIS DATA SET HAS BEEN RESTORED. ORIGINALLY THERE WAS ONE 9-TRACK, 1600 BPI TAPE. THERE IS ONE RESTORED TAPE. THE TAPE CONTAINS TWO FILES OF DATA, THE FIRST FILE IS ASCII AND THE SECOND FILE IS EBCDIC. THE TAPE WAS CREATED ON AN IBM 360 COMPUTER. THE DR TAPE IS A 3480 CARTRIDGE AND THE DS TAPE IS 9-TRACK, 6250 BPI. THE DR AND DS NUMBERS ALONG WITH THE CORRESPONDING D NUMBERS ARE AS FOLLOWS:

DR#	DS#	D#	FILES	TIME SPAN
DR03716	DS03716	D45319	2	09/01/77 - 03/09/78

HEAO 1

Extragalactic X-Ray Source Catalog

77-075A-02E

This data set has been restored. Originally there was one 9-track, 1600 BPI tape written in ASCII. There is one restored tape. The DR tape is a 3480 cartridge and the DS tape is a 9-track, 6250 BPI tape. The tape was created on a 3081 computer. The DR and DS numbers, along with the corresponding D number and the time span follow.

DR#	DS#	DD#	Files	Time Span
DR03672	DS03672	D48693	1	09/05/77 - 09/11/78

HEAO 1

SOURCE TARGET LIST, TIME & RA ORDERED

77-075A-02G

THIS DATA SET HAS BEEN RESTORED. ORIGINALLY THERE WAS ONE 9-TRACK, 6250 BPI TAPE WRITTEN IN EBCDIC WITH 3 BINARY HEADER RECORDS. THERE IS ONE RESTORED TAPE. THE DR TAPE IS A 3480 CARTRIDGE AND THE DS TAPE IS 9-TRACK, 6250 BPI. THE TAPE WAS CREATED ON AN IBM 3081 COMPUTER. THE DR AND DS NUMBERS ALONG WITH THE CORRESPONDING D NUMBER AND THE TIME SPAN IS AS FOLLOWS:

DR#	DS#	D#	FILES	TIME SPAN
DR03674	DS03674	D59881	1	11/15/77 - 12/29/78

X-406

D-45319

```
$EXE TPLIST BS

INPUT PARAMETERS ARE:  AS FL=1=1

 TAPE NO.   1               FILE NO.   1
 RECORD   1                 LENGTH   2480
                                                TABLE 2.
                                                                  LIST OF SOURCES.

                                                                             NAME        RA
L                 BOX1                          BOX2          SIZE 1  INT.  DAY       COMMENTS
                  DEC      B                1950  RA/DEC            1950  RA/DEC       SIZE 2
 1977                           (1)          (2)      (3)      (4)     (5)     (6)     (7)      (8)      (9)
 (10)    (11)   (12)    (13)   (14)        (15)

      H0008+105      2.12 107.12     4.97 359.39 359.16    4.75     1.67    1.44    2.57    2.79  3.30   1.6
4  362.     IIIZW2**                        10.54 -50.81    11.45    9.04    9.54   11.95    10.05  10.55
 11.04  10.53  0.64                      SAS3 POSITION
                                                                                  H0048-731      12.11 3
03.06   16.68   7.75   5.64  15.02   12.39  10.48  11.88  13.70  3.60   4.40  308.    SMCX-3**
                 -73.13 -44.27  -70.59 -76.02 -75.71 -70.36  -73.67 -73.41 -72.59 -72.85  0.54
              SAS3 POSITION
                                                       H0053-739     13.46 302.54   18.96  10.71   7
.75  16.68   14.48  11.76  12.52  15.15  4.80   4.70  307.   SMCX-2**                         -73.99
-43.41  -70.86 -76.39 -76.01 -70.59  -74.37 -74.06 -73.59 -73.91  0.40                   SAS3 POSITIO
N
                              H0111-149     17.87 146.87    15.35   21.03   20.77  15.11   17.10  16.8
4  18.65  18.90  3.60    1.49  367.    AB151*                          -14.93 -76.48  -16.31 -13.89 -1
3.34 -15.76  -15.59 -15.04 -14.27  -14.82  1.11


 TAPE NO.   1               FILE NO.   1
 RECORD   12                LENGTH   620


                                                                          NOTE 1:  THIS SOURCE CO
NFIRMED USING 3 DEGREE FOV.
  NOTE 2:  SOURCE NEAR NORTH ECLIPTIC POLE--NO BOX 2 DETERMINED.

***** JOB DONE.
$WEO LPS

$$
$REW LO
```

REQ. AGENT	RD #	ACQ. AGENT
LSM	V0088	MCL

HEAO 1

NEW HARD X RAY SOURCES

77-075A-02D

This data set consists of one data tape. It is 1600 bpi, 9 track with two files. The files are identical but the first file is in ASCII and the second file is in EBCDIC. This tape contains a listing of TABLE 2 of the paper " New Hard X-Ray Soures Observed with HEAO A2 ". The table contains the positions and intensities of these sources. The 'D' and 'C' numbers and time span follow:

D#	C#	TIME SPAN
D-45319	C-21559	9/1/77 - 3/9/78

77-075A-02D

Enclosure 1

The tape is 9 track, 1600 bpi. It contains two files which are identical except that the first is in ASCII and the second is in EBCDIC. The logical record size is 124 bytes. Each logical record is an image of a line normally printed on a line printer. The physical blocksize is 2480 bytes. The blocking format is FB.

Two lines of data are given for each source. The data are formatted as follows:

Line 1:

Columns	Format	Content
3	A1	'H'
4-7	I4	Right Ascension
8-11	I4	Declination
14-20	F7.2	Right Ascension
21-27	F7.2	Galactic Longitude
29-56	4F7.2	Right Ascension of Box 1
58-85	4F7.2	Right Ascension of Box 2
86-91	F6.2	Size of Error Box 1
92-98	F7.2	Intensity
99-104	F6.0	Day of Observation
109-124	16A1	Comments

Line 2:

Columns	Format	Content
14-20	F7.2	Declination
21-27	F7.2	Galactic Latitude
29-56	4F7.2	Declination of Box 1
58-85	4F7.2	Declination of Box 2
86-91	F6.2	Size of Error Box 2
109-124	16A1	Comments

DUMP OF TAPE X-406

INPUT TAPE X-406 ON MT2
DATA INPUT H9 FL 1 1 1

FILE 1 RECORD 1 LENGTH 2480BYTES

(0)	20202020	20202020	20202020	20202020	20202020	20202020	20202020	20202020	20202020	20202020
(40)	20202020	20202020	20205441	424C4520	322E2020	20202020	20202020	20202020	20202020	20202020
(80)	20202020	20202020	20202020	20202020	20202020	20202020	20202020	20202020	20202020	20202020
(120)	20202020	20202020	20202020	20202020	20202020	20202020	20202020	20202020	20202020	20202020
(160)	20202020	20202020	204C4953	54204F46	20534F55	52434553	2E202020	20202020	20202020	20202020
(200)	20202020	20202020	20202020	20202020	20202020	20202020	20202020	20202020	20202020	20202020
(240)	20202020	20202020	20202020	20202020	20202020	20202020	20202020	20202020	20202020	20202020
(280)	20202020	20202020	20202020	20202020	20202020	20202020	20202020	20202020	20202020	20202020
(320)	20202020	20202020	20202020	20202020	20202020	20202020	20202020	20202020	20202020	20202020
(360)	20202020	20202020	20202020	20202020	204E414D	45202020	20202020	52412020	20202020	4C202020
(400)	20202020	20202020	20202020	20424158	31202020	20202020	20202020	20202020	20202020	20202020
(440)	20204241	58322020	20202020	20202020	20205349	5A452031	2020494E	54452020	44415920	20202020
(480)	434F4D4D	454E5453	20202020	20202020	20202020	20202020	20202020	20202020	44454320	20202020
(520)	42202020	20202020	20202020	20203139	35302020	52412F44	45432020	20202020	20202020	20202020
(560)	20202031	39353020	2052412F	44454320	20202020	20205349	5A452032	20202020	20202020	31393737
(600)	20202020	20202020	20202020	20202020	20202020	20202020	20283129	20202020	20202020	28322920
(640)	20202028	33292020	20202020	28342920	20202028	35292020	20202836	29202020	20283729	20202020
(680)	20283829	20202020	28392920	20202831	30292020	20283131	29202028	31322920	20202831	33292020
(720)	28313429	20202020	20283135	29202020	20202020	20202020	20202020	20202020	20202020	20202020
(760)	20202020	20202020	20202020	20202020	20202020	20202020	20202020	20202020	20202020	20202020
(800)	20202020	20202020	20202020	20202020	20202020	20202020	20202020	20202020	20202020	20202020
(840)	20202020	20202020	20202020	20202020	20202020	20202020	20202020	20202020	20202020	20202020
(880)	20202020	20202020	20202020	20202020	20202020	20202020	20202020	20202020	20202020	20202020
(920)	20202020	20202020	20202020	20202020	20202020	20202020	20202020	20202020	20202020	20202020
(960)	20202020	20202020	20202020	20202020	20202020	20202020	20202020	20202020	20204830	3030382B
(1000)	31303520	20202020	322E3132	20313037	2E313220	20202034	2E393720	3335392E	33392033	35392E31
(1040)	36202020	342E3735	20202020	312E3637	20202031	2E343420	2020322E	35372020	20322E37	39202033
(1080)	2E333020	2020312E	36342020	3336322E	20202020	4949495A	57322A2A	20202020	20202020	20202020
(1120)	20202020	20202020	20202031	302E3534	202D3530	2E383120	20203131	2E343520	2020392E	30342020
(1160)	20392E35	34202031	312E3935	20202031	302E3035	20203130	2E353520	2031312E	30342020	31302E35
(1200)	33202030	2E363420	20202020	20202020	20202020	20202020	53415333	20504F53	4954494F	4E202020
(1240)	20202020	20202020	20202020	20202020	20202020	20202020	20202020	20202020	20202020	20202020
(1280)	20202020	20202020	20202020	20202020	20202020	20202020	20202020	20202020	20202020	20202020
(1320)	20202020	20202020	20202020	20202020	20202020	20202020	20202020	20202020	20202020	20202020
(1360)	20202020	20204830	3034382D	37333120	20202031	322E3131	20333033	2E303620	20203136	2E363820
(1400)	2020372E	37352020	20352E36	34202031	352E3032	20202031	322E3339	20203130	2E343820	2031312E
(1440)	38382020	31332E37	30202033	2E363020	2020342E	34302020	3330382E	20202020	534D4358	2D332A2A
(1480)	20202020	20202020	20202020	20202020	20202020	20202D37	332E3133	202D3434	2E323720	202D3730
(1520)	2E353920	2D37362E	3032202D	37352E37	31202D37	302E3336	20202D37	332E3637	202D3733	2E343120
(1560)	2D37322E	3539202D	37322E38	35202030	2E353420	20202020	20202020	20202020	20202020	53415333
(1600)	20504F53	4954494F	4E202020	20202020	20202020	20202020	20202020	20202020	20202020	20202020
(1640)	20202020	20202020	20202020	20202020	20202020	20202020	20202020	20202020	20202020	20202020
(1680)	20202020	20202020	20202020	20202020	20202020	20202020	20202020	20202020	20202020	20202020
(1720)	20202020	20202020	20202020	20202020	20204830	3035332D	37333920	20202031	332E3436	20333032
(1760)	2E353420	20203138	2E393620	2031302E	37312020	20372E37	35202031	362E3638	20202031	342E3438
(1800)	20203131	2E373620	2031322E	35322020	31352E31	35202034	2E383020	2020342E	37302020	3330372E
(1840)	20202020	534D4358	2D322A2A	20202020	20202020	20202020	20202020	20202020	20202D37	332E3939
(1880)	202D3433	2E343120	202D3730	2E383620	2D37362E	3339202D	37362E30	31202D37	302E3539	20202D37
(1920)	342E3337	202D3734	2E303620	2D37332E	3539202D	37332E39	31202030	2E343020	20202020	20202020
(1960)	20202020	20202020	53415333	20504F53	4954494F	4E202020	20202020	20202020	20202020	20202020
(2000)	20202020	20202020	20202020	20202020	20202020	20202020	20202020	20202020	20202020	20202020
(2040)	20202020	20202020	20202020	20202020	20202020	20202020	20202020	20202020	20202020	20202020
(2080)	20202020	20202020	20202020	20202020	20202020	20202020	20202020	20204830	3131312D	31343920
(2120)	20202031	372E3837	20313436	2E383720	20203135	2E333520	2032312E	30332020	32302E37	37202031
(2160)	352E3131	20202031	372E3130	20203136	2E383420	2031382E	36352020	31382E39	30202033	2E363020
(2200)	2020312F	34392020	3336372E	20202020	41423135	312A2020	20202020	20202020	20202020	20202020
(2240)	20202020	20202D31	342E3933	202D3736	2E343820	202D3136	2E333120	2D31332E	3839202D	31332E33
(2280)	34202D31	352E3736	20202D31	352E3539	202D3135	2E303420	2D31342E	3237202D	31342E38	32202D31

D-45319

```
(  2320)  2E313120  20202020  20202020  20202020  20202020  20202020  20202020  20202020  20202020  20202020
(  2360)  20202020  20202020  20202020  20202020  20202020  20202020  20202020  20202020  20202020  20202020
(  2400)  20202020  20202020  20202020  20202020  20202020  20202020  20202020  20202020  20202020  20202020
(  2440)  20202020  20202020  20202020  20202020  20202020  20202020  20202020  20202020  20202020  20202020

FILE      1  RECORD       12  LENGTH      620BYTES
(     0)  20202020  20202020  20202020  20202020  20202020  20202020  20202020  20202020  20202020  20202020
(    40)  20202020  20202020  20202020  20202020  20202020  20202020  20202020  20202020  20202020  20202020
(    80)  20202020  20202020  20202020  20202020  20202020  20202020  20202020  20202020  20202020  20202020
(   120)  20202020  20202020  20202020  20202020  20202020  20202020  20202020  20202020  20202020  20202020
(   160)  20202020  20202020  20202020  20202020  20202020  20202020  20202020  20202020  20202020  20202020
(   200)  20202020  20202020  20202020  20202020  20202020  20202020  20202020  20202020  20202020  20202020
(   240)  20202020  20202020  20202020  20202020  20202020  20202020  20202020  20202020  20202020  20202020
(   280)  20202020  20202020  20202020  20202020  20202020  20202020  20202020  20202020  20202020  20202020
(   320)  20202020  20202020  20202020  20202020  20202020  20202020  20202020  20202020  20202020  20202020
(   360)  20202020  20202020  20202020  204E4F54  4520313A  20205448  49532053  4F555243  4520434F  4E464952
(   400)  4D454420  5553494E  47203320  44454752  45452046  4F562E20  20202020  20202020  20202020  20202020
(   440)  20202020  20202020  20202020  20202020  20202020  20202020  20202020  20202020  20202020  20202020
(   480)  20202020  20202020  20202020  20202020  204E4F54  4520323A  2020534F  55524345  204E4541  52204E4F
(   520)  52544820  45434C49  50544943  20504F4C  452D2D4E  4F20424F  58203220  44455445  524D494E  45442E20
(   560)  20202020  20202020  20202020  20202020  20202020  20202020  20202020  20202020  20202020  20202020
(   600)  20202020  20202020  20202020  20202020  20202020

        FILE   INPUT    DATA RECORDS    MAX.         READ ERROR SUMMARY            INPUT RETRIES
               RECS.       INPUT        SIZE     PERM  ZERO B   SHORT  UNDEF.   #RECS.  TOTAL#
         1      12          13          2480      0      0        0      0        0       0

EOJ        DUMP STOPPED AFTER FILE   1         # OF PERMANENT READ ERRORS  0

START TIME 07/29/81  17:38:08         STOP TIME 07/29/81  17:38:18

$$
```

D45319

REQ. AGENT	RAND #	ACQ. AGENT
DAD	V0215	HKH

HEAO-1

SOURCE TARGET LIST, TIME & RA ORDERED

77-075A-02G

This data set contains one magnetic tape. It is 6250 BPI, 9 track, has 1 file and is written in EBCDIC with 3 binary header records, it was created on the 3081. The C tape is 1600 BPI.

D#	C#	TIME SPAN
D-59881	C-23463	11/15/77 - 12/29/78

G

July 20, 1983

TO: 601/Director (J. Vette)
National Space Science Data Center (NSSDC)

FROM: 660/HEAO-1 A2 Experiment
F. Marshall

SUBJECT: HEAO-1 A2 Data Submission

Enclosed are two lists of the targets that the HEAO A2 experiment pointed at during its mission. The lists are identical except that one is ordered by time and the other is ordered by right ascension of the y-axis. Each list has ten columns of information:

1) target name
2) whether the target was on the +y or -y side of the spacecraft (note that the A2 experiment only viewed the +y targets)
3) R.A. of y-axis (1950 epoch)
4) Dec. " "
5) Day of 1977 of start of point
6) Second " " " "
7) Day of 1977 of end of "
8) Second " " " "
9) 'PP' indicates spacecraft alternated between two positions during point.
10) point number

Also enclosed is a magnetic tape containing these lists and documentation on how to read the tape.

F.E. Marshall

Francis E. Marshall
Laboratory for High Energy Astrophysics

Enclosures

cc: E. Boldt/661
S. Holt/660

TWO PRINTED LISTS ≡ data on magnetic tape
⇒ only the 1st page of each list was preserved in this package. (CYN, 9/96)

77-075A-02G

Enclosure 1

The tape is 9 track, 6250 bpi and was written with the SACC IBM 3081. It contains one file which is copy of a partitioned data set containing two members. It can be read using the following JCLs:

```
// EXEC IEBCOPY
//SYSUT1 DD DSN=POINT.LIST,DISP=OLD,
//   LABEL=(1,NL,,IN),VOL=SER=XXXXX,
//   DCB=(DEN=4),UNIT=6250
//SYSUT2 DD DSN=ZBMEN.POINT.LIST,
//   DISP=SHR
//SYSUT3 DD SPACE=(1,10),UNIT=SYSDA
//SYSUT4 DD SPACE=(1,10),UNIT=SYSDA
//SYSPRINT DD SYSOUT=A
//SYSIN DD DUMMY
```

D-59881

```
                                  DUMP OF TAPE DOUT2

INPUT TAPE  DOUT2   ON  TU0
DATA INPUT    F9 FL 1 5 3

FILE     1  RECORD        1  LENGTH      60BYTES
(    0)  00300000  00380000  00C460FF  02001C70  00509000  00001C84  3050200B  00004A7D  0230001E  4B360103
(   40)  52080200  00000000  00000000  00000000  00000000

FILE     1  RECORD        2  LENGTH     284BYTES
(    0)  011C0000  01180000  01000000  FF000000  8F106644  04889A48  58002730  00000018  00040018  00080005
(   40)  00000000  00000000  00000000  00000000  00000000  00000000  00000000  00000000  00000000  00000000
(   80)  00000000  00000000  00000000  00000000  00000000  00000000  00000000  00000000  00000000  00000000
(  120)  00000000  00000000  00000000  00000000  00000000  00000000  00000000  00000000  00000000  00000000
(  160)  00000000  00000000  00000000  00000000  00000000  00000000  00000000  00000000  00000000  00000000
(  200)  00000000  00000000  00000000  00000000  00000000  00000000  00000000  00000000  00000000  00000000
(  240)  00000000  00000000  00000000  00000000  00000000  00000000  00000000  00000000  00000000  00000000
(  280)  00000000

FILE     1  RECORD        3  LENGTH     296BYTES
(    0)  01280000  01240000  00000000  00000000  00080100  FFFFFFFF  FFFFFFFF  0026E3C9  D4C54040  40400000
(   40)  0500E8C1  E7C9E240  40400002  0400FFFF  FFFFFFFF  FFFF0000  00000000  00000000  00000000  00000000
(   80)  00000000  00000000  00000000  00000000  00000000  00000000  00000000  00000000  00000000  00000000
(  120)  00000000  00000000  00000000  00000000  00000000  00000000  00000000  00000000  00000000  00000000
(  160)  00000000  00000000  00000000  00000000  00000000  00000000  00000000  00000000  00000000  00000000
(  200)  00000000  00000000  00000000  00000000  00000000  00000000  00000000  00000000  00000000  00000000
(  240)  00000000  00000000  00000000  00000000  00000000  00000000  00000000  00000000  00000000  00000000
(  280)  00000000  00000000  00000000  00000000

FILE     1  RECORD       13  LENGTH    7300BYTES
(    0)  1C840000  1C800000  00000000  00180008  01001C70  C7E7F3F0  F460F140  40404040  40404040  40404040
(   40)  4EE840F1  F9F44BF5  F64060F6  F14BF3F3  40F5F8F3  40404040  40F9F0F2  40F5F8F3  404040F2  F1F6F0F6
(   80)  40404040  40404040  40404040  F0F0F0F0  F0F2F4F4  C7E7F3F0  F460F140  40404040  40404040  40404040
(  120)  4EE840F1  F9F44BF5  F74060F6  F14BF3F7  40F4F1F1  404040F6  F1F0F8F0  40F4F1F1  404040F7  F2F9F6F0
(  160)  40404040  40404040  40404040  F0F0F0F0  F0F0F3F4  C7C1D4D4  C160C3C1  E2404040  40404040  40404040
(  200)  60E840F1  F9F54BF2  F94060F6  F14BF1F0  40F6F0F0  404040F1  F8F0F0F2  40F6F0F0  404040F4  F6F8F0F2
(  240)  40404040  40404040  40404040  F0F0F0F0  F0F2F7F4  F2C1F1F3  F0F660F0  F1F24040  40404040  40404040
(  280)  4EE840F1  F9F64BF5  F0404040  F14BF3F0  40F5F3F6  404040F5  F4F0F0F6  40F5F3F6  404040F7  F5F6F0F6
(  320)  40404040  40404040  40404040  F0F0F0F0  F0F1F6F8  C2C1C3D2  C7D9D6E4  D5C44040  40404040  40404040
(  360)  4EE840F1  F9F64BF8  F84040F1  F54BF0F8  40F7F2F7  404040F1  F0F7F3F9  40F7F2F7  404040F4  F8F6F0F8
(  400)  40404040  40404040  D7D74040  F0F0F0F0  F0F4F5F5  E5C9D9C7  D640C3D3  E4E2E3C5  D9404040  40404040
(  440)  4EE840F1  F9F74BF5  F04040F1  F54BF5F0  40F7F2F7  404040F1  F0F7F3F8  40F7F2F7  404040F4  F8F6F0F8
(  480)  40404040  40404040  D7D74040  F0F0F0F0  F0F4F5F4  F4E4F1F3  F1F44EF5  F9404040  40404040  40404040
(  520)  4EE840F1  F9F84BF4  F04040F5  F94BF5F0  40F4F9F9  404040F5  F7F6F0F6  40F4F9F9  404040F7  F9F2F0F6
(  560)  40404040  40404040  40404040  F0F0F0F0  F0F1F1F0  E2D4C340  E760F140  40404040  40404040  40404040
(  600)  60E840F1  F9F84BF9  F44040F7  F34BF7F8  40F7F1F0  404040F3  F4F2F0F2  40F7F1F0  404040F5  F7F6F0F6
(  640)  40404040  40404040  40404040  F0F0F0F0  F0F4F3F4  E2D4C340  E760F140  40404040  40404040  40404040
(  680)  60E840F1  F9F84BF9  F44040F7  F34BF7F8  40F7F1F4  404040F2  F1F6F0F2  40F7F1F4  404040F4  F3F2F0F6
(  720)  40404040  40404040  40404040  F0F0F0F0  F0F4F3F8  C3C5D540  C1404040  40404040  40404040  40404040
(  760)  4EE840F2  F0F04BF5  F54060F4  F24BF7F9  40F5F6F7  404040F6  F0F0F0F2  40F5F6F8  404040F1  F5F5F1F4
(  800)  40404040  40404040  D7D74040  F0F0F0F0  F0F2F2F2  C3C5D540  C1404040  40404040  40404040  40404040
(  840)  4EE840F2  F0F04BF6  F34060F4  F24BF7F8  40F3F8F4  404040F4  F6F0F2F7  40F3F8F4  404040F5  F7F9F5F9
(  880)  40404040  40404040  40404040  F0F0F0F0  F0F0F2F3  C140F2F3  F0404040  40404040  40404040  40404040
(  920)  60E840F2  F0F34BF9  F44040F1  F14BF7F5  40F5F6F0  40404040  F3F6F0F2  40F5F6F0  404040F2  F5F2F0F6
(  960)  40404040  40404040  40404040  F0F0F0F0  F0F2F1F0  C9C3F4F3  F2F9C140  40404040  40404040  40404040
( 1000)  4EE840F2  F0F64BF5  F44060F3  F04BF0F5  40F5F7F3  404040F6  F8F4F0F2  40F5F7F4  40404040  F3F6F0F2
( 1040)  40404040  40404040  40404040  F0F0F0F0  F0F2F3F2  F2C1F1F3  F4F64EF2  F6F54040  40404040  40404040
( 1080)  4EE840F2  F0F64BF7  F04040F2  F64BF7F0  40F5F4F3  40404040  F7F8F0F6  40F5F4F3  404040F4  F3F5F8F6
( 1120)  40404040  40404040  40404040  F0F0F0F0  F0F1F7F8  D4D240F2  F7F94040  40404040  40404040  40404040
( 1160)  4EE840F2  F0F74BF7  F54040F6  F94BF5F5  40F6F9F7  404040F3  F6F9F0F2  40F6F9F7  404040F6  F1F2F0F2
( 1200)  40404040  40404040  40404040  F0F0F0F0  F0F4F1F4  C2C1C3D2  C7D9D6E4  D5C44040  40404040  40404040
( 1240)  4EE840F2  F0F74BF9  F64040F6  F94BF5F5  40F6F9F4  404040F5  F2F2F0F2  40F6F9F5  404040F1  F4F4F0F8
( 1280)  40404040  40404040  D7D74040  F0F0F0F0  F0F4F1F0  F2C1F1F3  F4F84EF7  F0F04040  40404040  40404040
( 1320)  4EE840F2  F0F74BF9  F74040F6  F94BF3F5  40F6F9F4  404040F5  F2F2F0F2  40F6F9F5  404040F1  F4F4F0F8
```

3 header records

4-10

11|15|77

77-075A-02G

Listed by NSSDC Staff

```
$ASS IN TU1
$NOP
$NOP
$NOP ********** DOUT-2 ***********
$EXE TPLIST DS

INPUT PARAMETERS ARE:  ED SR=4=1 1

 TAPE NO.   1                FILE NO.   1
 RECORD   4                  LENGTH   7500
 d                    TEST POINT         +Y 167.25  59.00 319   16933 319   28794            0000000
1SMCX-1             +Y  19.20 -73.60 320    64338 320    76360                00000002CYG X-1
  +Y 299.12  35.06 321   67621 321   79677              00000003A754               +Y 135.70  -9.50
322   76939 323    2302              00000004VELA P             +Y 308.70  45.10 327   69403 327   8
0C84              00000005MK421                 -Y 345.88 -38.27 333   59273 333   69936           000
00006VELA PULSAR           +Y 128.70 -45.10 335   54041 335   64606              00000007NGC4151
    +Y 182.00  39.80 340   46299 340   57016             000000082A0922               +Y 140.50 -31
.70 341   43746 341   54326             00000009SS CYGNI             +Y 325.18  43.36 350     7446 350
  19480              00000010BLLAC               -Y 149.11 -42.13 355   63198 355   77620
 00000011 3C273               -Y   7.18  -2.08 356   60538 356   74972              00000012M87
        -Y   7.61 -12.42 357   57849 357   72146              00000013M87                  +Y 187.01
 12.66 362   70454 362   82405             00000014HZ43                 +Y 278.30 -23.22 363   67780
 363   79667            000000154U0050-01           +Y  12.63  -1.99 369   57443 369   69262
    00000016NGC3783               +Y 174.28 -37.51 370   54601 370   66537             000000173C279
           -Y  13.40   5.52 374   61336 374   72268              00000018UVCETI                 +Y  2
4.00 -18.22 375   58794 375   69562             00000019CEN X-3             +Y 169.76 -60.35 378   5
0754 378   62465            00000020NOVA(3U0115+63)      +Y  18.80  63.47 381   48368 381   59013
      00000021CAS A              +Y 350.30  58.55 382   51551 382   62161             00000022CE
N A              +Y 200.63 -42.78 384   46027 384   57959             00000023GX301-2               +
Y 185.92 -62.49 390   46198 390   58060             00000024M 31               -Y 190.01 -41.00 396
  64501 396   76447             00000025GX301-2             +Y 185.95 -62.49 397   67661 397   8204
3          00000026GX301-2               -Y   5.95  62.49 398   70967 398   85217             000000
27CEN A               -Y  21.48  43.08 399   62223 399   76567             000000284U0336+01
  +Y 034.50 000.53 402   59915 402   74126              00000029TYCHO               -Y 185.60 -63.88
 403   57030 403   71372              00000030A 401               +Y  43.65  13.25 404   54247 404
68660             00000031NGC 1275              +Y  49.15  41.35 405   51493 405   65779             00
000032A 401             -Y 223.96 -13.31 410    3236 410   14582             00000033GX304-1
    +Y 194.57 -61.37 411   61080 411   72960              00000034TYCHO               +Y   5.60  6
3.88 412   64440 412   76074             00000035CIR X-1              +Y 229.20 -56.99 413   67440 41
3   79320              00000036A1540-53              +Y 235.30 -53.40 416   59053 416   70814
 00000037NGC 1275            -Y 228.72 -41.26 417   56294 417   67940              00000038A1439-61
            +Y 219.80 -61.45 418   65262 418   75854             00000039UX ARI              +Y  50.8
8  28.54 419   56490 419   73025              00000040HER X-1              +Y 254.01  35.42 420   5386
3 420   65542             00000041HER X-1              +Y 254.01  35.42 423   57297 423   67806
   00000042HER X-1              +Y 254.01  35.42 424   59237 424   70893             000000433C120
            -Y 247.94  -5.31 425   58561 425   68090             00000044MSH14-63               +Y 2
19.05 -61.21 426   53460 426   65337             00000045MK 501             -Y  73.31 -41.83 427
52810 427   64744          PP  00000046MK 501             -Y  72.63 -39.90 427   52810 427   64744
     PP  00000047HER X-1             +Y 254.01  35.42 430   48011 430   59819             00000048H
ER X-1            +Y 254.01  35.42 431    2707 431   16650              00000049MXB 1728-34
+Y 262.20 -33.80 432   66058 432   77199             00000050MXB 1728-34            -Y  82.20  33.80 43
3   68340 433   80176              00000051MXB 1729             262.20 -33.80 434   66299 434   773
38          00000052MXB 1659-29            -Y  75.75  29.90 438   65986 438   77849             00000
053MXB 1728-34            -Y  82.20  33.80 439   63071 439   83320             000000544L1626-67
   -Y  67.11  67.63 440   66227 440   80461              000000554U0517+17              +Y  80.00  17.6
0 444   66601 445    6348              000000564U1700-37              +Y 254.14 -38.34 445   73806 445
 84606             000000573C129               +Y 251.35 -44.95 446   57606 446   74109        PP  0
00000588ACKGROUND             +Y 250.90 -46.94 446   57606 446   74109        PP  000000594U1700-37
     +Y 254.14 -38.34 447   72183 447   84152              00000060CRAB(4U0531+21)     +Y  84.46
21.95 448   64806 449    1806              00000061GX1+4               +Y 262.20 -24.70 452    1802 4
52   18307             00000062AMHER              +Y 273.74  49.85 452   50402 452   72007            P
P  00000063BACKGROUND           +Y 274.49  43.87 452   50402 452   72007          PP  000000644U1626-6
7          +Y 246.60 -67.38 453   55806 453   77406             00000065H1743-32              +Y 265.
```

77-075A-02G

Provided by P.I.

**** TSO FOREGROUND HARDCOPY ****
DSNAME=ZBMEN.POINT.LIST

(TIME)

TEST POINT	+Y	167.25	59.00	319	16933	319	28794		00000001
SMCX-1	+Y	19.20	-73.60	320	64338	320	76360		00000002
CYG X-1	+Y	299.12	35.06	321	67621	321	79677		00000003
A754	+Y	135.70	-9.50	322	76939	323	2302		00000004
VELA P	+Y	308.70	45.10	327	69403	327	80084		00000005
MK421	-Y	345.88	-38.27	333	59273	333	69936		00000006
VELA PULSAR	+Y	128.70	-45.10	335	54041	335	64606		00000007
NGC4151	+Y	182.00	39.80	340	46299	340	57016		00000008
2A0922	+Y	140.50	-31.70	341	43746	341	54326		00000009
SS CYGNI	+Y	325.18	43.36	350	7446	350	19480		00000010
BLLAC	-Y	149.11	-42.13	355	63198	355	77620		00000011
3C273	-Y	7.18	-2.08	356	60538	356	74972		00000012
M87	-Y	7.61	-12.42	357	57849	357	72146		00000013
M87	+Y	187.01	12.66	362	70454	362	82405		00000014
HZ43	+Y	278.30	-23.22	363	67780	363	79667		00000015
4U0050-01	+Y	12.63	-1.99	369	57443	369	69262		00000016
NGC3783	+Y	174.28	-37.51	370	54601	370	66537		00000017
3C279	-Y	13.40	5.52	374	61586	374	72268		00000018
UVCETI	+Y	24.00	-18.22	375	58794	375	69562		00000019
CEN X-3	+Y	169.76	-60.35	378	50754	378	62465		00000020
NOVA(3U0115+63)	+Y	18.80	63.47	381	48368	381	59013		00000021
CAS A	+Y	350.30	58.55	382	51551	382	62161		00000022
CEN A	+Y	200.63	-42.78	384	46027	384	57959		00000023
GX301-2	+Y	185.92	-62.49	390	46198	390	58050		00000024
M 31	-Y	190.01	-41.00	396	64501	396	76447		00000025
GX301-2	+Y	185.95	-62.49	397	67661	397	82043		00000026
GX301-2	-Y	5.95	62.49	398	70967	398	85217		00000027
CEN A	-Y	21.48	43.08	399	62223	399	76567		00000028
4U0336+01	+Y	054.50	000.53	402	59915	402	74126		00000029
TYCHO	-Y	185.60	-63.88	403	57030	403	71372		00000030
A 401	+Y	43.65	13.25	404	54247	404	68660		00000031
NGC 1275	+Y	49.15	41.35	405	51493	405	65779		00000032
A 401	-Y	223.96	-13.31	410	3236	410	14582		00000033
GX304-1	+Y	194.57	-61.37	411	61080	411	72960		00000034
TYCHO	+Y	5.60	63.88	412	64440	412	76074		00000035
CIR X-1	+Y	229.20	-56.99	413	67440	413	79320		00000036
A1540-53	+Y	235.30	-53.40	416	59053	416	70814		00000037
NGC 1275	-Y	228.72	-41.26	417	56294	417	67940		00000038
A1439-61	+Y	219.80	-61.45	418	65262	418	75854		00000039
UX ARI	+Y	50.88	28.54	419	56490	419	73025		00000040
HER X-1	+Y	254.01	36.42	420	53863	420	65642		00000041
HER X-1	+Y	254.01	35.42	423	57297	423	67806		00000042
HER X-1	+Y	254.01	35.42	424	59237	424	70893		00000043
3C120	-Y	247.94	-5.31	425	58561	425	68090		00000044
MSH14-63	+Y	219.05	-61.21	426	53460	426	65337		00000045
MK 501	-Y	73.31	-41.83	427	52810	427	64744	PP	00000046
MK 501	-Y	72.63	-39.90	427	52810	427	64744	PP	00000047
HER X-1	+Y	254.01	35.42	430	48011	430	59819		00000048
HER X-1	+Y	254.01	35.42	431	2707	431	16650		00000049
MXB 1728-34	+Y	262.20	-33.80	432	66058	432	77199		00000050
MXB 1728-34	-Y	82.20	33.80	433	68340	433	80176		00000051
MXB 1729		262.20	-33.80	434	66299	434	77338		00000052
MXB 1659-29	-Y	75.75	29.90	438	65986	438	77849		00000053
MXB 1728-34	-Y	82.20	33.80	439	63071	439	83320		00000054
4U1626-67	-Y	67.11	67.63	440	66227	440	80461		00000055
4U0517+17	+Y	80.00	17.60	444	66601	445	6348		00000056
4U1700-37	+Y	254.14	-38.34	445	73806	445	84606		00000057
3C129	+Y	251.35	-44.95	446	57606	446	74109	PP	00000058
BACKGROUND	+Y	250.95	-46.94	446	57606	446	74109	PP	00000059
4U1700-37	+Y	254.14	-38.34	447	72183	447	84152		00000060
CRAB(4U0531+21)	+Y	84.46	21.98	448	64806	449	1806		00000061
GX1+4	+Y	262.20	-24.70	452	1802	452	18307		00000062
AMHER	+Y	273.74	49.85	452	50402	452	72007	PP	00000063
BACKGROUND	+Y	274.49	43.87	452	50402	452	72007	PP	00000064
4U1626-67	+Y	246.60	-67.38	453	55806	453	77406		00000065
H1743-32	+Y	265.60	-32.65	454	57816	454	75652		00000066
MXB 1730-32(BURSTER)	+Y	262.53	-33.35	455	64806	455	71645		00000067
JUPITER	-Y	268.49	-23.36	457	78604	458	03488	PP	00000068
JUPITER	-Y	268.47	-25.36	457	78604	458	03488	PP	00000069
3C390.3	-Y	101.55	-80.00	458	46322	458	59408	PP	00000070
4U1847+78	-Y	103.31	-80.09	458	46322	458	59408	PP	00000071
CG195+4	+Y	100.00	17.50	459	49926	459	72248	PP	00000072
CG195+4	+Y	98.00	17.50	459	49926	459	72248	PP	00000073
LMCX-1	+Y	085.10	-69.8	461	42512	461	64800	PP	00000074
LMC X-3	+Y	084.70	-64.10	461	42512	461	64800	PP	00000075
3C390.3	-Y	101.55	-80.00	465	46328	465	57606	PP	00000076
4U1847+78	-Y	98.31	-78.09	465	46328	465	57606	PP	00000077
2A1914-589	+Y	289.20	-58.82	466	31927	456	64808	PP	00000078
2A1914-589	+Y	291.20	-65.10	466	31927	466	64808	PP	00000079

**** TSO FOREGROUND HARDCOPY ****
DSNAME=ZBMEN.POINT.LIST

(YAXIS)

77-075A-02G
Provided by P.I.

MKN335	+Y	1.80	20.50	553	72003	554	32033	PP	00000199
4U0009-33	+Y	1.85	-34.02	516	36002	516	57606		00000135
NGC 4151	-Y	2.35	-39.63	522	10446	522	32408	PP	00000143
2A1102+384	-Y	2.35	-39.65	514	14406	514	36002		00000131
NGC 4151	-Y	2.35	-39.63	526	10876	526	32348	PP	00000149
NGC 4151	-Y	3.00	-40.45	526	10876	526	32348	PP	00000150
NGC 4151	-Y	3.00	-40.45	522	10446	522	32408	PP	00000144
TYCHO	+Y	5.60	63.88	584	28801	584	61207		00000246
TYCHO	+Y	5.60	63.88	412	64440	412	76074		00000036
GX301-2	-Y	5.95	62.49	398	70967	398	85217		00000027
3C273	-Y	6.80	-2.30	548	35882	548	57607		00000188
3C273	-Y	6.80	-2.30	543	43586	543	64507		00000179
3C273	-Y	6.82	-2.35	556	63002	557	9003		00000204
3C273	-Y	7.18	-2.08	356	60538	356	74972		00000012
M87(VIRGO)	-Y	7.23	-12.58	531	72006	532	7202		00000160
M87	-Y	7.60	-12.60	539	46806	539	68402		00000172
M87	-Y	7.61	-12.42	367	57849	367	72146		00000013
A 85	+Y	9.78	-9.63	547	16206	547	55806		00000186
M31	+Y	10.01	41.00	568	54002	568	72002		00000224
4U0050-01	+Y	12.63	-1.99	369	57443	369	69262		00000016
3C279	-Y	13.40	5.52	374	61586	374	72268		00000018
GAMMA CAS	+Y	13.41	60.40	584	8101	584	28801		00000245
3C279	-Y	13.70	5.65	559	57602	560	3602		00000209
2A0054-015	+Y	13.73	-1.53	558	54901	559	12606		00000208
XGAL HOLE	+Y	14.19	-0.44	734	43202	735	25209	PP	00000469
COMA	-Y	14.70	-28.04	542	28806	542	68106		00000177
H0106-15	+Y	16.60	-15.68	550	1203	550	25322		00000191
2A1308+32	-Y	17.32	-32.46	557	9003	557	30607		00000205
1308+32	-Y	17.40	-32.50	540	46806	540	68106		00000174
CEN A	-Y	18.33	40.88	571	67923	572	3609	PP	00000230
NOVA(3U0115+63)	+Y	18.80	63.47	381	48368	381	59013		00000021
4U0115+63	+Y	18.81	63.48	566	51602	566	73202		00000220
SMC X-1	+Y	18.83	-73.70	502	28806	502	50406		00000114
SMC X-1	+Y	18.83	-73.70	500	43206	500	64806		00000111
SMCX-1	+Y	19.20	-73.60	320	64338	320	76360		00000002
BACKGROUND	-Y	19.59	44.50	582	17522	582	61206	PP	00000243
XGAL HOLE	+Y	19.73	-13.32	734	43202	735	25209	PP	00000468
2A0120-353	+Y	20.23	-35.30	526	72006	527	7202		00000151
BACKGRDND	-Y	20.54	47.90	578	35522	578	79208	PP	00000237
CEN A	-Y	21.48	43.08	399	62223	399	76567		00000028
CEN A	-Y	22.28	40.28	578	35522	578	79208	PP	00000236
CEN A	-Y	23.34	43.88	582	17522	582	61206	PP	00000242
?		23.34	43.88	589	18002	589	31484		00000255
UVCETI	+Y	24.00	-18.22	375	58794	375	69562		00000019
CEN A	-Y	25.32	46.22	571	67923	572	3609	PP	00000229
NCG5506	-Y	32.99	3.07	572	64802	573	6		00000231
NGC 5506	-Y	32.99	3.07	565	72602	566	9606		00000219
MKN 590	+Y	33.00	-1.00	564	57002	564	78601		00000216
NGC 554	-Y	34.24	-25.22	560	54002	561	3		00000211
4U0223+31	+Y	35.95	31.28	584	85502	585	22502		00000247
BACKGROUND	+Y	36.66	39.96	607	85922	608	34988	PP	00000288
2A0251+413	+Y	42.20	41.38	589	31484	589	50406		00000256
BACKGROUND	+Y	42.70	40.16	607	21602	607	51308	PP	00000286
NGC 1129	+Y	42.98	41.38	607	85922	608	34988	PP	00000287
A 401	+Y	43.65	13.25	404	54247	404	68660		00000031
4U1456+22	-Y	44.50	-22.47	575	28802	575	82807		00000234
	-Y	46.63	-6.93	593	10802	593	32402		00000261
2A0311-227	+Y	47.91	-22.78	565	49202	565	72602		00000218
2A0316-443	+Y	49.05	-44.31	561	45902	562	2706		00000213
4U0316+41(PERSEUS)	+Y	49.11	41.37	607	21602	607	51308	PP	00000285
NGC 1275	+Y	49.15	41.35	405	51493	405	65779		00000032
3U1516-56	-Y	49.20	56.99	608	72002	609	18002		00000289
CIR X-1	-Y	49.20	56.99	738	54002	738	72090		00000476
CIR X-1	-Y	49.78	57.09	612	75602	613	27007		00000296
UX ARI	+Y	50.88	28.54	419	56490	419	73025		00000040
NGC 1365	+Y	52.95	-36.30	738	79463	739	10806		00000477
2A0335-096	-Y	53.83	9.63	593	79202	594	14402		00000263
2A0343-532	+Y	55.80	-53.60	534	64806	534	86346		00000166
2A0343-536	+Y	55.82	-53.63	551	79202	552	18002		00000195
PKS 0349-14	+Y	57.30	-13.94	588	14402	588	36002		00000254
X-PER	+Y	58.06	30.90	599	13924	599	36012	PP	00000272
A2142	-Y	59.22	-27.37	581	7202	581	50406		00000241
A 2147	-Y	60.56	-16.41	585	79622	586	37208	PP	00000249
BACKGROND	-Y	60.78	-16.93	585	79622	586	37208	PP	00000250
3C120	+Y	62.74	4.15	615	54002	616	8	PP	00000300
A 478	+Y	62.81	10.39	602	39602	602	53106		00000279
3C111	+Y	63.75	37.90	611	10323	611	43508	PP	00000292
BACKGROUND	+Y	63.81	31.85	599	13924	599	36012	PP	00000273
4U1626-67	-Y	67.11	67.63	440	66227	440	80461		00000055

REQ. AGENT	RAND #	ACQ. AGENT
DAD	V0215	HKH

HEAO-1

EXTRAGALACTIC X-RAY SOURCE CATALOG

77-075A-02E

This data set contains one magnetic tape. It is 1600 BPI, 9 track, written in ASCII, has 1 file and was created on the 3081. The time span is not found on the tape but, is contained in the documentation.

D#	C#	TIME SPAN
D-46893	C-23462	9/05/77 - 9/11/78

ENCLOSURE 1

The tape is 9 track, 1600 bpi. It contains one file which is in ASCII. The logical record size is 120 bytes. Each logical record is an image of a line normally printed on a line printer. The physical blocksize is 2400 bytes. The blocking format is FB.

B33286-000H
DLO=X
HCK=D

71-01511-020

NASA

Technical Memorandum 82168

A Complete X-Ray Sample of the High Latitude (|b| > 20°) Sky from HEAO -1 A-2: Log N - Log S and Luminosity Functions

G. Piccinotti, R. F. Mushotzky, E.A. Boldt,
S. S. Holt F. E. Marshall, P. J. Serlemitsos
and R. A. Shafer

AUGUST 1981

National Aeronautics and
Space Administration

Goddard Space Flight Center
Greenbelt, Maryland 20771

A COMPLETE X-RAY SAMPLE OF THE HIGH LATITUDE ($|b|>20^{o}$) SKY FROM HEAO-1 A-2: LOG N - LOG S AND LUMINOSITY FUNCTIONS

G. Piccinotti[1], R.F. Mushotzky, E.A. Boldt, S.S. Holt,

F.E. Marshall, P.J. Serlemitsos and R.A. Shafer[2]

Laboratory for High Energy Astrophysics

NASA/Goddard Space Flight Center

Greenbelt, Maryland 20771

ABSTRACT

The HEAO-1 experiment A-2 has performed a complete X-ray survey of the 8.2 steradians of the sky at $|b| > 20^{o}$ down to a limiting sensitivity of $\lesssim 3.1 \times 10^{-11}$ ergs/cm^2 sec in the 2-10 keV band. Of the 85 detected sources (excluding the LMC and SMC sources) 17 have been identified with galactic objects, 61 have been identified with extragalactic objects and 7 remain unidentified. The log N - log S relation for the non-galactic objects is well fit by the Euclidean relationship. We have used the X-ray spectra of these objects to construct log N - log S in physical units. The complete sample of identified sources has been used to construct X-ray luminosity functions, using the absolute maximum likelihood method, for clusters of galaxies and active galactic nuclei.

Keywords: X-Ray Sources, Luminosity Function, Cosmic X-Ray Background

[1]NAS/NRC Research Associate

[2]Also Dept. Physics & Astronomy, Univ. of Maryland

I. INTRODUCTION

The HEAO-1 satellite experiment A-2 (Rothschild et al. 1979) with its extended energy range, complete sky coverage, low and stable internal background and moderate spatial resolution has enabled us to create a complete catalog of X-ray sources at galactic latitudes $|b| > 20^o$ down to a limiting sensitivity of 3.1×10^{-11} ergs/cm^2 sec in the 2-10 keV band. Recent identifications of these sources by modulation collimator experiments on HEAO-1 and SAS-3 as well as imaging detectors on HEAO-2 has resulted in certain identifications of all sources of flux $\gtrsim 4.0 \times 10^{-11}$ ergs/cm^2 sec, pending confirmation of two clusters and NGC 7172, and reasonable identifications for 78 out of the 85 (92%) sources in the sample. All but 9 of these identifications are extremely likely or certain. This identification ratio for the extragalactic sources compares to identification of 45 out of 67 (67%) sources in the sample of Warwick and Pye (1979).

The completeness of this sample enables construction of the number-intensity distribution (log N - log S) for X-ray sources as well as developing X-ray luminosity functions for clusters of galaxies and active galactic nuclei. In addition the body of X-ray spectral data returned by A-2 allows us to cast the log N - log S distribution in absolute rather then instrument dependent units which enables comparison with the log N - log S relation in different X-ray energy bands (cf. Giacconi et al. 1979).

Analysis of this data shows that the source counts are well fit by a "Euclidean" law with

$$\frac{dN}{dS} = 16.5\ S^{-5/2}\ (\text{R15 cts/sec})^{-1}\ \text{sr}^{-1}$$

consistent with previous results despite the quite different samples (Warwick and Pye 1978; Schwartz 1979). The luminosity functions are well fit by power law representations with

$$\frac{dN}{dL_{44}} \lesssim 3.5 \quad 10^{-7} \; L_{44}^{-2.15} \; (10^{44} \text{ erg/sec})^{-1} \; \text{Mpc}^{-3}$$

for clusters of galaxies, and

$$\frac{dN}{dL_{44}} \lesssim 2.7 \times 10^{-7} \; L_{44}^{-2.75} \; (10^{44} \text{ erg/sec})^{-1} \; \text{Mpc}^{-3}$$

for active galactic nuclei, similar to previous results (McKee et al. 1980; Pye and Warwick 1979). Integration of the luminosity functions over the $\lesssim 10^{42.5} - 10^{45}$ erg/sec range within which they are well determined results in estimates of the contribution of clusters and active galactic nuclei to the integral 2-10 keV unresolved X-ray background of $\lesssim$ 4% for clusters and $\lesssim$ 20% for active galaxies. Using these luminosity functions, with no evolution, we estimate that $\lesssim$ 30% of the sources seen in the Einstein Observatory deep survey (Giacconi et al. 1979) should be relatively low luminosity ($L < 1 \times 10^{44}$ erg/sec) nearby ($z \lesssim 0.5$) objects.

II. DATA ANALYSIS AND SOURCE SELECTION

The HEAO-1 A-2 experiment, described in detail by Rothschild et al. (1979), provided two independent, low background, high sensitivity surveys of the entire sky six months apart. We have analyzed the A-2 data in order to obtain a complete flux limited sample of extragalactic X-ray sources. The region between -20° and $+20^{\circ}$ in galactic latitude has been excluded to minimize contamination from galactic sources. A circle of 6 degrees radius around the LMC sources has been also excluded to prevent confusion problems. Therefore, we remain with 65.5% of the sky (8.23 ster). The statistical significance of the existence of the sources is tested by determining the decrease in χ^2 when the new source is added to the model. All sources in the sample give a decrease in χ^2 of at least 30. The probability of having, by chance, a decrease of 30 in χ^2 with two degrees of freedom (scan angle and intensity) is 3×10^{-7}. This probability is almost the same as the one associated with a deviation of 5σ in a Gaussian distribution (6×10^{-7}). Therefore, we can also state that the lowest statistical significance for the existence of the sources included in our sample is 5σ, as required by the maximum likelihood methods we use to determine the log N - log S parameters (see Section IV-1). Taking into account this statistical significance requirement we estimated the completeness level of the first and the second scan as 1.25 and 1.8 R15 counts/sec respectively, see Figure 1. One R15 count/sec $\lesssim$ 2.17 erg cm^{-2} sec^{-1} in the 2-10 keV energy band for a power law spectrum with photon index 1.65. R15 is a counting rate derived using the $1.5^{\circ} \times 3^{\circ}$ FWHM fields of view of the second layer of the argon counter and both layers of a xenon counter. This combination has a FWHM for the quantum efficiency from $\lesssim$ 3 to $\lesssim$ 17 keV (Marshall et al. 1979).

The second pass is less sensitive on average, because much more time was spent in pointing at sources. We shall be more concerned with the first pass data in deriving best fit parameters and use the second pass ones mostly as an independent confirmation.

III. OBSERVATIONS

A. The Sample

Table 1 contains all the relevant data for the 68 sources either brighter than 1.25 R15 c/s in the first scan which corresponds to days 248-437 of 1977, or brighter than 1.8 in the second scan, days 73-254 of 1978. Source names are listed in column 1. Column 2 contains previous catalog names.

First pass fluxes and 1σ errors are in column 3, while the second pass ones are in column 4. Some fluxes may differ slightly from previously reported results, as different procedures have been used; e.g., in the recent paper by McKee et al. (1980) fluxes have been obtained fixing the X-ray position at the optical position, instead here we have used the best fit X-ray position to derive the flux. Available identifications are listed in column 5. The type of object is in column 6. One * in column 7 indicates firm identifications (i.e. as provided by the SAS-3 or HEAO-1 modulation collimators or by the Einstein X-ray telescope), two * indicates possible identification consistent with larger error boxes. Redshift values and references are given in column 8. Spectral information is now available for more than half of our sources (Mushotzky et al. 1980; Worrall et al. 1980; Mushotzky 1979; Holt 1980; Boldt 1980), we quote in column 9 conversion factors between R15 counts/s and ergs cm^{-2} s^{-1}. When spectral information is lacking we assumed a 6 keV thermal bremsstrahlung spectrum for all sources identified with clusters and a 1.65 photon index power law for all sources identified with active galaxies. An average conversion factor value of 2.5 x 10^{-11} ergs cm^{-2} s^{-1}/R15 counts s^{-1} was assumed for the few unidentified sources. Columns 10 and 11 contain the first and second pass luminosities in units of 10^{44} erg s^{-1} calculated for H_o = 50 km/s/Mpc and q_o = 0.5. Column 12 contains notes.

B. Classes of Sources

Sixty of the 82 sources brighter than 1.25 counts s^{-1} in the first scan and not definitely associated with galactic objects have been associated with extragalactic objects. Only 7 remain unidentified at the present time. These 60 identified sources subdivide almost equally between clusters of galaxies (30) and single galaxies (30). Most of the 30 galaxies are Seyfert galaxies of class 1 or 2, but we have also 1 QSO (3C 273), 4 BL Lac objects, and 1 "normal" galaxy (NGC 7172). Note that M31 and the Magellanic Cloud sources are not included in our extragalatic sample because they represent a local inhomogeneity as part of the local group of galaxies. Table 2 lists the 17 high galactic latitude sources not included in our extragalactic sample because they have been identified with galactic or "local" objects. The second pass sample contains only 37 sources brighter than 1.8 Ri5 counts/sec, all but one identified. The source classification is consistent with the first pass. Assuming Poisson errors, clusters contribute 50 ± 9% of the identified sources in the first pass and 61 ± 13% in the second. Galaxies contribute 50 ± 9% in the first scan and 39 ± 10% in the second.

C. New Sources and Sample Completeness

H0328+025 and H0917-075 are the only entirely new sources in Table 1. Figure 2 shows their error boxes. All the other sources in Table 1 have been listed somewhere else before. The improvement in our sample, as compared to previously reported ones, is due to a better rejection of non-extragalactic sources, made possible by the recent identifications, and to a uniform sky coverage to a relatively low limiting flux.

As the instrument has a fairly large (1.5^{o} x 3.0^{o}) angular resolution the possibility of source confusion must be considered. The total area of the sky included in this survey is approximately 2.7 x 10^4 square degrees, therefore there are about 6 x 10^3 independent positions on it. As the high galactic latitude X-ray sources bright enough to give confusion problems at our sensitivity level cannot be more than a hundred using the log N-log S relation derived later (taking into account also the possibility that two weaker sources can simulate a source bright enough to be included in our list) we therefore expect negligible confusion. That is using $\frac{dN}{dS} \leq 16.5\ S^{-1.5}$ there are roughly 65 resolution elements per source, of S > 1.25 cts, well above the confusion level of 25 beam areas per source often quoted in the literature. In addition the uniform sky coverage at the chosen sensitivity levels provided by this experiment and the availability of two independent sets of data for cross-checking purposes support our confidence in the completeness of our sample.

D. Space Distribution of Sources

Since the pioneering work of DeVaucouleurs (1958) much attention has been devoted to finding evidence of a supercluster centered in the Virgo cluster of galaxies. We plotted the positions of our sources in supergalactic coordinates looking for some kind of anisotropy. Figure 3 shows the 1st pass sample. Obviously, no anisotropy is observed as most sources lie beyond the supercluster. If we restrict our attention to the 12 sources with redshifts less than .01 (in boxes in Figure 3), we see that 9 are in the center region of the supercluster while 3 are in the anticenter and that all but one have supergalactic latitude less than 30 degrees in absolute value This result, which is significant at the few percent level, suggests that close X-ray galaxies may lie preferentially in the supergalactic plane. But no conclusion can safely be made from such a small number of objects at present.

IV. THE NUMBER-FLUX FUNCTION

The usual power law form

$$N(S) = KS^{-\alpha} \quad (\text{R15 counts/sec})^{-1}\text{sr}^{-1} \qquad (1)$$

has been assumed for the number-flux relation. The various methods applied to estimate the coefficient K and the differential exponent α as well as to evaluate the goodness of the fit are outlined in the next section.

A. Statistical Methods

1. Maximum Likelihood

Crawford, Jauncey and Murdoch applied the maximum likelihood method to unbinned data in order to estimate the slope of the number-flux relation of radio sources. In the first paper (Crawford et al. (1970) a solution is worked out for error free data. In the second paper (Murdoch et al. 1973) the method is extended to include errors on the measured fluxes. Numerical corrections to the error free answers were calculated for the special case of Gaussian distributed errors. In the same paper it was pointed out that a minimum signal-to-noise ratio of five is required so that the uncertainty in the correction factor due to weaker sources does not dominate the correction itself. This is why we excluded from our sample sources with statistical significance less than 5σ. In both Papers I and II the Kolmogorov-Smirnov test (here after: K-S test) was suggested to evaluate the goodness of the fit obtained. In the remainder of this paper we will refer to this method as to the Maximum Likelihood (ML) method.

2. Absolute Maximum Likelihood

The ML method assumes the same underlying error distribution for all the souces in the sample, i.e. it assigns the same 1σ error to all the sources. As we deal with sources of greater than 5σ significance the error assumed is one fifth of the minimum flux in the sample, or .25 R15 counts s^{-1} in the first scan and .36 R15 counts s^{-1} in the second. Table 1 shows that these values are not very far from the actual errors. However Lightman et al. (1980) have developed a refinement of the ML method in connection with the K-S test capable of handling sources with their own experimental error. Following those authors we will call this new statistical method the "Absolute Maximum Likelihood" (AML) method. Lightman et al. (1980) worked out the AML method on general grounds and then applied it to the evaluation of globular cluster

X-ray source masses. As this is the first application of the AML method to the number flux function, we give a short outline of the method below. Assuming the form (1) for the number-flux relation and a Gaussian form $\rho(F_i,\sigma_i,S)$ for the error distribution of the measured fluxes we evaluated numerically the integral probabilities $\overset{<}{P}_i(\alpha)$ as

$$\overset{<}{P}_i(\alpha) = \frac{\int_{F_{min}}^{F_i} dF \int_{F_{co}}^{\infty} dS\ N(S,\alpha)\ \rho(F,\sigma_i,S)}{\int_{F_{min}}^{\infty} dF \int_{F_{co}}^{\infty} dS\ N(S,\alpha)\ \rho(F,\sigma_i,S)} \qquad (2)$$

where S is the true flux, F_i and σ_i are the measured flux and error of the i-th source. F_{CO} is a cutoff value used to avoid the apparent divergence at $F = 0$. As in Murdoch et al. (1973) the particular choice of the cutoff value does not affect the value of the integral as long as the statistical significance of the sources is at least 5σ. F_{min} is the sensitivity limit of the sample. For every assumed α we computed the $\overset{<}{P}_i(\alpha)$ for all the sources. The $\overset{<}{P}_i(\alpha)$ should be uniformly distributed between 0 and 1. Following Lightman et al. we evaluated the maximum deviation from the uniform distribution:

$$D_{max}(\alpha) = \max_{i=1,N} [D_i(\alpha)] = \max_{i=1,N} \left(\left|\overset{<}{P}_i(\alpha) - \frac{i}{N}\right|\right) \qquad (3)$$

where N is the number of sources in the sample and the $\overset{<}{P}_i(\alpha)$ have been sorted in ascending order. Then we calculate the probability $P(D_{MAX}(\alpha))$ of observing deviations greater than $D_{MAX}(\alpha)$ from the formula for the K-S statistic given by Birnbaum and Tingey (1951). The $(\alpha, P(D_{max}(\alpha))$ function is then plotted. The best fit value of α is the one corresponding to the maximum value P_{MAX} of the $P(D_{max}(\alpha))$ distribution. Obviously P_{MAX} must be greater than some minimum value (say 10%) in order to accept the model. The range in α for results given below on α are evaluated from the values α_1 and α_2 of α, which reduce $P(D_{max}(\alpha))$ to $P_{MAX}/2$.

3. Chi-Square

Both the ML and the AML methods are independent of the coefficient κ of the number-flux relation, as κ is lost in normalizing the probabilities. Therefore, we used the χ^2 method to determine κ. Bins with equal expected number of sources for $\alpha = 2.5$ have been used for the χ^2 calculations. Of course, in calculating confidence bounds, we have assumed that the functional form of the distribution is the "true" one. If better data later shows that this is not true our confidence values are not applicable.

V. LOG N - LOG S RESULTS

The ML method applied to the 60 non-galactic sources brighter than 1.25 R15 counts s^{-1} in the first pass gives (in this section we use R15 counts s^{-1} as the unit)

$$\alpha = 2.67 \pm .23$$

with a goodness of fit probability (evaluated using the KS test) of 39.5 percent.

For the 37 non-galactic sources brighter than 1.8 R15 counts s^{-1} in the second pass the ML result is

$$\alpha = 2.74 \pm .32$$

with a probability of 17.5 percent.

The AML results are

$$\alpha = 2.63 \pm .2$$

in the first pass, see Figure 4a, and

$$\alpha = 2.74 \pm .22$$

in the second, see Figure 4b.

The 68 and 95 percent probability contours for the 1st pass values of κ and α evaluated with the χ^2 method are plotted in Figure 4c The χ^2 best fit values and 1σ errors for the number-flux function parameters are

$$\alpha = 2.72^{-.10}_{+.15} \qquad (4)$$

$$\kappa = 20^{-2.6}_{+4.0} \quad (\text{R15 counts/sec})^{\alpha-1}\ \text{sr}^{-1}.$$

The differential number-flux data as well as the best fit function

$$N(S) = 20\ S^{-2.72} \quad (\text{R15 counts/sec})^{-1}\ \text{sr}^{-1}$$

are plotted in Figure 5; the χ^2 value of the fit is 2.79 for 6 degrees of freedom, corresponding to a probability $P(> \chi^2) \lesssim 83\%$. The limited size of the second scan sample does not allow a good estimate of the probability but the results are consistent with the first pass ones.

C. Number Flux Relation in Physical Units

Using the conversions factors listed in column (9) of Table 1 we can express the fluxes in ergs cm^{-2} s^{-1} and evaluate the number-flux relation accordingly. Conversion factors range approximately from 2.0×10^{-11} to 2.9×10^{-11} ergs cm^{-2} s^{-1} (R15 counts $s^{-1})^{-1}$, the highest values referring to soft spectra sources whose emission peak lies below our instrument energy window. As a consequence of the different conversions factors the completeness level of the samples when fluxes are in ergs cm^{-2} s^{-1} is equal to the former completeness level in R15 counts s^{-1} times the maximum conversion factor: that is $< 3.6 \times 10^{-11}$ ergs cm^{-2} s^{-1} for the first pass and 5.2×10^{-11} ergs/cm^2 sec in the second pass. The 1st scan sample with this flux restriction contains 51 sources: 25 clusters, 22 "galaxies" and 4 unidentified sources. The best fit values and 1 σ errors for the number-flux function parameters obtained with the three methods agree with

$$\alpha \lesssim 2.85 \pm .3$$
$$\kappa \lesssim (5.65^{-1.3}_{+1.9}) \times 10^{-19} \; (\text{ergs cm}^{-2}\text{s}^{-1})^{\alpha-1}\text{sr}^{-1} \qquad (5)$$

The 32 second scan sources brighter than 5.2×10^{-11} ergs cm^{-2} s^{-1} give us a best fit of slightly steeper slope $\alpha \lesssim 3.1 \pm .4$.

VI. DISCUSSION OF THE RESULTS

All the first pass samples, whether fluxes are expressed in R15 counts s^{-1} or in ergs cm^{-2} s^{-1} are consistent with the five halves Euclidean slope (see Figures 6 and 7). The slight preference for a steeper than Eucledian slope is due to the distribution of the brightest few sources in calculating the likelihood functions. It is these sources that are most sensitive to changes in α by virtue of the relatively small statistical error in their measured intensity. Our Euclidean best fit for the 1st pass data is

$$N(S) = 16.5^{+3}_{-2}\ S^{-2.5}\ (\text{R15 counts/s})^{-1}\text{sr}^{-1}$$

with a χ^2 of 5.5 for 7 degrees of freedom; $\rho(\chi^2 > 5.5) \lesssim 60\%$. The AML probability for $\alpha = 2.5$ is 42.4%. Assuming an average conversion factor of 2.4 x 10^{-11} ergs $cm^{-2}s^{-1}$ (R15 counts s)$^{-1}$ the relation (4) becomes

$$N(S) \lesssim (1.9^{+.35}_{-.25}) \times 10^{-15}\ S^{-2.5}\ (\text{ergs cm}^{-2}\text{s}^{-1})^{-1}\ \text{sr}^{-1}$$

in agreement with the exact result

$$N(S) \lesssim (2.2^{+.3}_{-.2}) \times 10^{-15}\ S^{-2.5}\ (\text{ergs cm}^{-2}\text{s}^{-1})^{-1}\ \text{sr}^{-1}$$

obtained from the 1st pass complete sample for fluxes in ergs $cm^{-2}s^{-1}$ and using the conversion factors in Table 1.

VII. COMPARISON WITH PREVIOUS EXPERIMENTS

Both the Uhuru (Schwartz 1979) and Ariel 5 data (Warwick and Pye 1978) gave a flux-number function consistent with the Euclidean model. Their best fit values for the coefficient κ with $\alpha = 2.5$ and S in R15 counts s^{-1} are respectively

$\kappa = 16.5 \pm 3.9$ using 1 Uhuru ct/s = 1.0 R15 ct/sec

and

$\kappa = 15.8 \pm 4.2$ using 1 Ariel-5 ct/sec = 2.12 R15 ct/sec

in agreement with our results at the 1σ level. These conversion factors assume a mean R15 conversion factor of 2.4 x 10^{-11} ergs/sec, 1 Uhuru ct/sec = 2.4 x 10^{-11} erg/sec, and 1 Ariel-5 count/sec = 5.1 x 10^{-11} erg/sec. If we use the calibration of Marshall et al. (1979) appropriate for the active galaxies of 1 R15 ct/sec = 2.17 x 10^{-11} erg/cm^2 sec, we find $\kappa_{Uhuru} \lesssim 20$ and

$\kappa_{Ariel-5} \lesssim 19$. The best fit slope of Warwick and Pye of 2.7 ± .2 is also consistent with our result.

VIII. LUMINOSITY FUNCTION

A. Method and Data Base

Many authors (Schwartz 1978; McHardy 1978; McKee et al. 1980; Elvis et al. 1977; Pye and Warwick 1979; Tananbaum et al. 1978; Boldt 1980) have recently considered the problem of evaluating the X-ray luminosity functions for different classes of sources principally, clusters of galaxies and active galaxies. All of them with the exception of Pye and Warwick had to rely upon optical data to select complete samples. We present here X-ray luminosity functions evaluated from X-ray flux limited samples. As we remain with a few unidentified sources, our results have some uncertainty, but we believe that the residual incompleteness should not be very important.

1. The Samples

The first pass sample of clusters of galaxies contains 30 objects. The second pass one includes 22 sources. Thirty "galaxies" are observed in the first pass, but we exclude from our sample the QSO 3C273, the 4 BL Lac objects, the peculiar galaxy M82 and the "normal" galaxy NGC 7172 as they are not homogeneous with the bulk of the sample which consists of Seyfert galaxies. Therefore we remain with 23 active galactic nuclei. The second pass sample contains only 12 objects (after excluding 3C 273 and PKS 2155-304).

The completeness of the sample is checked using the Schmidt $\langle V/V_M \rangle$ test and with a K-S test on the distribution of the V_i/V_{M_i} as suggested by Avni and Bahcall (1980). The results are listed in Table 3.

TABLE 3

CLASS OF OBJECTS	SCAN #	# OBJECTS IN SAMPLE	$\langle V/V_M \rangle$	K-S TEST P(>d) %
Clusters of Galaxies	1	30	.471±.054	18.1
Clusters of Galaxies	2	22	.552±.062	11.8
Active Galaxies	1	24	.523±.059	50.4
Active Galaxies	2	12	.557±.083	56.8

The 1σ error quoted for $\langle V/V_M \rangle$ is the formal error $1/\sqrt{12N}$, where N is the number of objects in the sample (see Avni and Bahcall). All the 4 samples meet the requirements of the tests. However, we expect a small degree of incompleteness due to the unidentified sources.

2. Methods of Analysis

Of the three methods outlines in Sec (IV-A) only the AML is suited for the determination of the luminosity function parameters. The relatively small sizes of the samples do not allow an efficient use of the χ^2 square method or of any other binned method. Moreover the ML method in the form developed by Crawford, Jauncy and Murdoch cannot be used because of its assumptions of a single underlying error distribution. This last hypothesis was reasonably satisfied by the flux data in the evaluation of the log N log S parameters, as we already pointed out, but is not satisfied at all by the luminosity data, as the errors are proportional to the square of the redshift of the sources:

$$\sigma_{L_i} \approx z_i^2 \, \sigma_{F_i} \qquad (6)$$

On the contrary the AML method is well suited for the task. The description of Section IV-A still applies. However, instead of calculating the probabilities of eq (2) we evaluated the probabilities:

$$\hat{P}_i(q) = \frac{\int_0^{L_i} dL' \int_{L_{min}}^{L_{max}} dL\ f(L,q)\ V_{max}(L,F_{min})\ \rho(L,\sigma_{L_i}, L')}{\int_0^{\infty} dL' \int_{L_{min}}^{L_{max}} dL\ f(L,q)\ V_{max}(L,F_{min})\ \rho(L,\sigma_{L_i}, L')} \qquad (7)$$

Eq. (7) gives the integral normalized probabilities of observing a source with measured luminosity less or equal to L_i, assuming a Gaussian error distribution with standard deviation σ_{L_i}, and for the differential luminosity function the form f(L,q) where L is the true luminosity and q represents the functional parameters to be determined. L_{min} and L_{max} are the lower and upper boundaries of the luminosity function. V_{MAX} is the maximum volume at which one could detect the source and depends on the sensitivity limit of the sample. For a source of luminosity L in a sample of minimum sensitivity F_{MIN} the maximum visibility volume V_{MAX} is proportional to $(\sqrt{L/F_{min}})^3$ Note that Eq. (7) does not take in account errors on the redshift z. The AML method can determine the form of the luminosity function but not its absolute value. Therefore we have used a least squares fit to the unbinned data to evaluate the multiplicative coefficient.

B. Results

1. Clusters of Galaxies Luminosity Function

We considered two different forms for the luminosity function: the power law form

$$f(L) = KL^{-\gamma}$$

and the exponential form

$$f(L) = Ke^{-L/L_o}$$

between the minimum (L_{44min}) and maximum (L_{44max}) observed luminosities, expressed in units of 10^{44} ergs sec^{-1}. The normalization for a power law luminosity function scales as H_o^{-1}.

Clusters of Galaxies

Figure 9 represents the AML probabilities for the slope of the cluster of galaxies power law luminosity function. The 1st pass best fit values for the power law parameters are

$$\gamma = 2.15^{+.12}_{-.17}$$
$$K = (3.5 \pm 1.1) \times 10^{-7} \quad (10^{44}\ erg/s)^{\gamma-1}\ Mpc^{-3}.$$

K has been evaluated with the least squares method. The error on K has been determined by letting γ assume the 1σ extreme values of 2.03 and 2.32. Figure 8a gives a binned representation of the data with the best fit luminosity function. Each bin contains three sources, except for the highest luminosity bin which contains five. The second pass results are

$$\gamma = 2.13^{+.16}_{-.24}$$
$$K = (3.8 \pm 2) \times 10^{-7} \quad (10^{44}\ ergs/s)^{\gamma-1}\ Mpc^{-3}$$

Figure 8b give the binned representation. The minimum luminosity object in both the 1st and the 2nd pass at 2.4×10^{43} (ergs/s) is the Virgo cluster. The highest luminosity cluster is Abell 2142 with 2.8×10^{45} (ergs/s).

The exponential form of the luminosity function has also been considered, but the quality of the fit is poorer, see Figure 10.

As the Virgo Cluster of galaxies has a "local" character, we evaluated the cluster of galaxies luminosity function without the Virgo cluster. The 1st pass sample is reduced to 29 sources, the mean V/V_{MAX} is 0.486 ± 0.055 and the K-S text on the uniformity of the V/V_{MAX} distribution gives a probability of 24.7%. The 2nd pass sample contains 21 sources, the mean V/V_{MAX} is 0.576 ± .063 and the K-S probability is 6.1%. Figure 9 gives the usual $(\gamma, P(\gamma))$ probability curves for the power law slope. The best fit values for the parameters are

1st scan
$$\gamma = 2.03 \pm .18$$
$$K = (2^{+1.2}_{-.8}) \times 10^{-7} \quad (10^{44}\ \mathrm{ergs/s})^{\gamma-1}\ \mathrm{Mpc}^{-3}$$

2nd scan
$$\gamma = 2.07^{+.2}_{-.25}$$
$$K = (3.2 \pm 2) \times 10^{-7} \quad (10^{44}\ \mathrm{ergs/s})^{\gamma-1}\ \mathrm{Mpc}^{-3}.$$

The minimum luminosity is now $\leq 3.6 \times 10^{43}$ ergs/s (Abell 1060) in both first and second scan. The exponential fit is again poorer, see Figure 10.

2. Active Galaxies

i. Luminosity Function

The insert in Figure 11 represents the AML probability for the power law slope of the active galaxies differential luminosity function calculated from the 1st pass data. The best fit values for the power law parameters are:

$$\gamma = 2.75 \pm .15$$
$$K = (2.7 \pm .15) \times 10^{-7} \quad (10^{44}\ \mathrm{ergs/s})^{\gamma-1}\mathrm{Mpc}^{-3}$$

NGC 3227 is the weakest source in the sample with 1.75×10^{42} ergs/s and

IIIZw2 is the brightest with 1.3 x 10^{45} ergs/s. Figure 11 shows the binned representation (3 sources/bin). This result is similar to that of Boldt (1980) and Pye and Warwick (1979). The exponential form for the luminosity function is not acceptable as the probabilities are always less than 2%.

The second pass sample is too small for a good determination of the luminosity function, however we find power law slopes steeper but consistent with the first pass ones

ii. A Lower Limit to the Active Galaxy Luminosity Function

The active galaxies contribution to the cosmic X-ray background depends strongly on the lower luminosity limit of the luminosity function. The lower luminosity limit for which the function can represent the data, L_{44MIN}, can be calculated by noting that the luminosity function must be consistent with the log N - log S observations. Namely, we can set a lower limit on L_{44MIN} by requiring that the number of active galaxies brighter than 1.25 R15 counts/sec expected from the luminosity function does not exceed the observed number plus 1 or 2 times the square root of the expected number.

From eq (14.7.35) of Weinberg (1972), and assuming a power law luminosity function we have (for $\gamma \neq 2.5$ and $\gamma \neq 3$)

$$N(>S) \simeq KA \left[\frac{1}{2.5-\gamma} \left[L^{2.5-\gamma}\right]_{L_{MIN}}^{L_{MAX}} S^{-3/2} - \frac{B}{3-\gamma} \left[L^{3-\gamma}\right]_{L_{MIN}}^{L_{MAX}} S^{-2}\right] \qquad (8)$$

where: S is the flux in ergs $cm^{-2}s^{-1}$

K and γ are the parameters of the differential power law luminosity function in Mpc^{-3} $(erg/sec)^{-(\gamma-1)}$

L_{MAX} and L_{MIN} are the upper and lower limit of the luminosity function (actually N(>S) depends strongly on L_{MIN} and very weakly on L_{MAX})

all the luminosities are in ergs/s

$A \simeq 3.20 \times 10^{-75}$

$B \simeq 4.7 \times 10^{-29}$ (assuming H_o = 50 km/s/Mpc)

N(>S) is the total number of sources in the sky uncorrected for sky coverage. The second term of this equataion represents a first order cosmological correction to the Eucledian result.[1]

....

(1) Footnote:

For L in units of 10^{44} erg/sec equation (8) has constants

$A = 3.2 \times 10^{-9}$

$B = 2.3 \times 10^{-7}$ $(H_o/50)$ $(1+\Gamma)$ where Γ is the spectral index of the source (here chosen to be .7)

....

Assuming an average conversion factor of 2.17×10^{-11} ergs $cm^{-2}s^{-1}$ per R15 counts s^{-1} we find that the 1σ lower limit on L_{MIN} is 4×10^{42} when γ is 2.75 and K is 2.68×10^{-7} $(10^{44}$ ergs/s$)^{-1}$ Mpc^{-3} and L_{MAX} varies between 5 and 15 x 10^{44} ergs/sec.

In Table 4 we show the 1 and 2σ limits on L_{MIN} as a function of L_{MAX} and γ. We note that we have not included in Table 4 the possibility that all (or some) of the unidentified sources could be Seyfert galaxies. However, considering the distribution of identified sources with flux < 3 R15 cts/sec, we would expect, at most, 3 of these unidentified objects to be active galaxies.

TABLE 4

APPROXIMATE L_{MIN} FOR VALUES OF L_{MAX} AND γ

$L_{MAX} = 1.5 \times 10^{45}$	$L_{MAX} = 3 \times 10^{45}$

	γ				γ	
	2.6	2.75	2.9	2.6	2.75	2.9
1σ	1.5×10^{42}	2.5×10^{42}	4.5×10^{42}	1.5×10^{42}	3.0×10^{42}	4.5×10^{42}
2σ	4.5×10^{41}	1.5×10^{42}	2.5×10^{42}	5.5×10^{41}	1.5×10^{42}	3.0×10^{42}

C. Discussion

1. Clusters of Galaxies

We note that our luminosity function for clusters of galaxies is very similar to the result of McKee et al. (1980). This indicates that, whatever selection effects are operating in making a X-ray or optically complete sample, they do not strongly bias the result. However there is a strong overlap in the individual objects between this sample and McKee's. The method we have used has allowed us in principle to discriminate between exponential and power law luminosity functions for clusters. It is somewhat surprising that a power law is favored, since it requires a change in form at low luminosities in order not to exceed the space density of all clusters (Bahcall 1979). However, the contribution of clusters to the diffuse X-ray background (DXRB) depends only weakly on the lower limit chosen. We do remind the reader that an exponential form is not excluded. Our data are not capable of rejecting the exponential form. They are also not capable of determining well the three constants in Bahcall's (1979) suggested form of the luminosity function.

Keeping in mind that the mean X-ray spectrum of clusters differs significantly from the diffuse X-ray background we shall, for historical reasons, compare the 2-10 keV volume emissivity of clusters to that of the diffuse X-ray background. For $q_o = 1/2$, $H_o = 50$ km/sec/Mpc the 2-10 keV background has a volume emissivity of $\lesssim 2.4 \times 10^{39}$ erg/sec/Mpc^3. The contribution of clusters is

$$\int_{L_{MAX}}^{L_{MIN}} f(L)\, LdL \lesssim 1 \times 10^{38} \text{ ergs/sec/Mpc}^3$$

(for $L_{MAX} = 3 \times 10^{45}$ ergs/sec, $L_{MIN} = 1 \times 10^{43}$ ergs/sec, where we have used the 1st pass cluster power law luminosity function without the Virgo cluster). Therefore, in an average sense, clusters contribute $\lesssim$ 4% of the 2-10 keV background. (For a more accurate treatment of the problem which includes the effect of the spectral differences of clusters from the background see McKee et al. 1980 and Marshall et al. 1980). We note that the present value agrees well with the estimate made by Marshall et al. (1980) of the maximum possible contribution of clusters if they were not to distort the thermal bremsstrahlung fit to the spectrum of the DXRB in the 3-50 keV band. We note that the relatively soft spectra of clusters should result in an increase in their contribution to the DXRB in the Einstein Observatory energy range.

2. Active Galaxies

The luminosity function derived here is in reasonable agreement with those derived previously by Pye and Warwick (1979) and Boldt (1980) in both slope and normalization. Using a lower bound of 3.0×10^{42} ergs/sec and a upper bound of 1.5×10^{45} erg/sec for our luminosity function results in a volume emissivity of $\lesssim 4.9 \times 10^{38}$ ergs/sec Mpc^3 or a contribution of $\lesssim$ 20% to the 2-10 keV DXRB. If the lower limit is 1.2×10^{42} (see Table 4) the contribution to the DXRB is $\lesssim$ 40%. In fact, in order not to exceed the DXRB the luminosity function of AGN's must flatten at $L \gtrsim 3 \times 10^{41}$ ergs/sec (De Zotti 1980). There is a strong indication of such a flattening in the optical luminosity function (Huchra and Sargent 1973; Huchra 1977; Huchra 1980) at

$M_V \lesssim - 21.5$ (H_o =50) equivalent to a optical bolometric luminosity of $\lesssim 1.2 \times 10^{44}$ ergs/sec. Since the slope of the optical luminosity function, at higher luminosities, is the same, within errors, (Huchra and Sargent 1973; Weedman 1979) as the X-ray function it is tempting to associate the bend in the optical luminosity function with the bend in the X-ray function and therefore derive a $L_{opt}/L_X \lesssim 35$. This value is rather larger than that found by examing individual objects (Kriss et al. 1980; Elvis et al 1978). This may be due to the fact that most of the optical flux from low luminosity active galaxies does not come from the nucleus but from the stellar population.

The total space density of X-ray emitting active galaxies in the luminosity range $3 \times 10^{42} - 1.5 \times 10^{45}$ is $\lesssim 7 \times 10^{-5}$ Mpc^{-3} which is $\lesssim 1.5\%$ of all galaxies of $M_p < -19$ (Huchra 1977). This compares to a space density of active galaxies of $M_p < -19$ of $\lesssim 5 \times 10^{-5}$ Mpc^{-3} (Huchra 1977, 1980). It thus seems, to first order, that all active galaxies of $M_p < -19$ emit X-rays at $L_x > 3 \times 10^{42}$ ergs/sec. For a flat universe there are (assuming no evolution) $\lesssim 4 \times 10^7$ X-ray emitting active galaxies with $L_x > 3 \times 10^{42}$ with $z \lesssim 3.5$.

We can also estimate, the number of sources per square degree expected in the Einstein deep survey if the luminosity function used in this paper does not evolve strongly in either slope or norm and that spectral effects, such as low energy absorption, are not important. With $q_o = .5$, $L_{min} = 3 \times 10^{42}$ in the 2-10 keV band and, $S_{min} = 5 \times 10^{-14}$ ergs/cm^{2}sec in the 2-10 keV band, (which corresponds to the Einstein "deep survey" limit for a $\alpha = 0.7$ source we predict $\lesssim 6$ active galaxies per square degree and $\lesssim 1.3$ clusters per square degree, compared to the 19 ± 8 total sources per square degree seen by the Einstein Observatory (Giacconi et al. 1979). DeZotti (1980) has performed a similar calculation and finds $\lesssim 5$ active galaxies per square degree for L_{min} =

9.1×10^{41} and $L_{max} = 2.9 \times 10^{44}$ ergs/sec in the 2-6 keV band and assuming that the slope of the luminosity function is 2.5. Since most of the objects are near L_{min} we would expect many of the Einstein survey objects to be Seyfert galaxies of $L_x \lesssim 5 \times 10^{42}$ erg/sec and $z \lesssim .20$. This is a consequence of the well known fact that if the luminosity function is steeper than 2.5, and barring strong evolution, when one looks at fainter objects one is looking primarily lower in the luminosity function rather than at higher redshift objects.

A simple way to look at the problem is to examine the number of objects predicted by our best fit luminosity function which would have redshifts (z) $\lesssim 0.5$ and would have luminosities high enough to have been included in the Einstein Deep Survey. (We shall use $q_o = .5$ or 0 geometry for simplicity). For $S_{min} = 5 \times 10^{-14}$ ergs/cm^2 sec in the 2-10 keV band and $q_o = .5$ that we predict $< 1.4 \times 10^4$ sources/ster due to active galaxies and $< 1.4 \times 10^3$ sources/ster due to clusters compared to the $6.3 \pm 2.6 \times 10^4$ sources/ster seen in the deep survey (Giacconi et al. 1979). We therefore predict that $< 25\%^{+17}_{-8}$ of the sources in the deep survey are low ($L \lesssim 4 \times 10^{43}$) close by ($z \lesssim .5$) active galaxies or clusters of galaxies of luminosity $> 1 \times 10^{43}$ erg/sec. That this was a likely situation was noted by Fabian and Rees (1978). (If $q_o = 0$ the number of sources increases to $< 2.1 \times 10^4$ sources/ster and the calculated contribution to the Einstein source counts to $35^{+24}_{-11}\%$).

Both the contribution of active galaxies to the DXRB and their contribution to the Einstein source counts depend sensitively on the lower limit, L_{min}, of the luminosity function used. It is possible that the luminosity where the flattening of the luminosity function takes place could be higher than our calcuated value if we allow a two slope model of the luminosity function rather than our simple single slope power law model with a cutoff. However our data are not good enough to constrain such a model. We therefore strongly caution the reader that these results are model dependant and should be treated as such.

IX. CONCLUSIONS

We have performed an all sky survey of X-ray sources complete to a limiting sensitivity of 3.1×10^{-11} ergs/cm^2 sec in the 2-10 keV band. Of the 85 detected sources only 7 remain without reasonable identifications. The log N- log S relation for extragalactic sources is well fit by a Euclidean law $\frac{dN}{dS} = 16.5\ S^{-2.5}$ where S is in R15 ct/sec or $\frac{dN}{dS} = 2.2 \times 10^{-15}\ S^{-2.5}\ (\mathrm{erg/cm^2 s})^{-1}\ \mathrm{sr}^{-1}$ where S is in erg/cm^{2}s in the 2-10 keV band. This complete sample has allowed construction of luminosity functions based on a flux limited sample for clusters of galaxies and active galactic nuclei. These functions are well represented by power laws of slope 2.05 and 2.75 respectively. The sample enables us to estimate that the luminosity function for active galaxies should flatten at $L \lesssim 3 \times 10^{42}$ erg/sec in the 2-10 keV band. The space density of X-ray emitting active galaxies is approximately the same as that of optically selected Seyfert galaxies.

Integration of the best fit luminosity functions indicates that clusters of galaxies contribute $\leq$ 4% of the 2-10 keV diffuse X-ray background and active galactic nuclei $\leq$ 20%. The sum of these contributions is very similar to the 26±11% contribution due to resolved due to sources seen in the Einstein deep survey. We also predict that many of the objects seen in the deep survey should be local, ($z < 0.5$), relatively low luminosity active galactic nuclei and clusters of galaxies. In order to determine more accurately the contribution of low luminosity active galaxies to the diffuse X-ray background one would have to sample the luminosity range $10^{41-42.5}$ over large solid angles. This would require a complete sky survey with $\leq$ 30 times the sensitivity of the present one and a angular resolution $\lesssim$ 20 times better. Such a survey would also extend the luminosity function up to luminosities of $\lesssim 10^{47}$ ergs/sec. We stress the importance of a complete unbiased X-ray survey with good identifications in determining log N - log S and luminosity functions since there are various classes of sources of widely varying X-ray to optical luminosities. We feel that this strategy rather then deep observations over small solid angles will determine log N - log S and the luminosity functions most accurately for the local epoch since for a given observing time and fixed instrumental parameters the number of observed sources greater than some statistical limit is maximized when the solid angle is maximized at a given completeness level for a photon limited experiment.

ACKNOWLEDGMENTS

We thank J. Swank for extensive discussions and her major contribution to the HEAO-1 analysis program. We thank J. Huchra, D. Schwartz, W.H.M. Ku and C. Forman-Jones for communicating results prior to publication and G. DeZotti and T. Maccacaro for interesting discussion and D. Schwartz for a careful reading of the manuscript.

TABLE 1

(1)	(2)	(3)	(4)	(5)	(6)	(7)	(8)	(9)	(10)	(11)	(12)
HØØØ8+1Ø5	2SØØØ7+1Ø7	1.64 .21	<1.35	IIIZW2	1	*	.Ø898 W3	2.175	12.9		
HØØ39-Ø96	2AØØ39-Ø96 4UØØ37-1Ø	2.64 .24	3.21 .38	ABELL 85	6	*	.Ø499 HSM	2.5ØØ	7 .25	8.82	
HØØ54-Ø15	2AØØ54-Ø15 4UØØ5Ø-Ø1	1.74 .33	2.13 .35	ABELL 119	6	*	.Ø446 N	2.55Ø	3.89	4.76	
HØ111-149		1.49 .22	.93 .35		7			2.5ØØ			1
HØ122-591	2AØ12Ø-591 4UØ1Ø6-59	1.29 .18	1.38 .2	FAIRALL9	1	*	.Ø461 W3	2.175	2.63	2.81	
HØ123-352	2AØ12Ø-353 4UØ115-36	2.52 .19	1.Ø4 .28	NGC526A	1	*	.Ø18 W3	2.175	.772	.319	
HØ2Ø6-Ø19	HØ2Ø6-Ø19	1.34 .23	.87 .41	MKN59Ø	1	*	.Ø27 W1	2.175	Ø.91	Ø.59	
HØ235-52	2AØ235-52	2.12 .14	.99 .23		7						
HØ256+134	2AØ255+132 1MØ254+132 4UØ254+13	2.95 .24	3.Ø3 .33	ABELL 4Ø1	6	*	.Ø748 H	2.48Ø	18.3	18.8	
HØ316-443	2AØ316-443 4UØ321-45	1.82 .19	1.Ø7 .23	PKSØ316-443	6	**	.Ø9 MA	2.52Ø	16.7	9.82	
HØ335+Ø96	2AØ335+Ø96 4UØ344+11	1.14 .22	1.86 .35	Ø335+Ø96	6	*	.Ø4 SC	2.81Ø	2.25	3.67	
HØ342-538	2AØ343-536 1MØ328-524 4UØ339-54	1.4 .16	1.42 .17	CAØ342-538	6	*	.Ø52 MQ	2.52Ø	4.21	4.27	
HØ411+1Ø4	2AØ411+1Ø3 1MØ4Ø5+1ØØ 4UØ41Ø+1Ø	2.61 .3	2.66 .34	ABELL 478	6	*	.Ø9 B	2.48Ø	23.6	24.Ø	
HØ43Ø-616	2AØ43Ø-615 1MØ426-635 4UØ427-61	2.53 .11	2.88 .14	SERSIC4Ø/6	6	*	.Ø6Ø1 V	2.48Ø	1Ø.1	11.4	
HØ431-134	2AØ431-136 4UØ431-12	2.16 .29	1.73 .3	ABELL 496	6	*	.Ø36 C2	2.52Ø	3.Ø9	2.48	
HØ43Ø+Ø53	2SØ43Ø+Ø5 4UØ432+Ø5	2.Ø4 .25	1.53 .36	3C12Ø	1	*	.Ø33 DV	2.175	2.12	1.59	
HØ548-322	1MØ545-322 4UØ543-31	1.7 .18	1.2 .25	PKSØ548-322	3	*	.Ø69 FD	2.675	9.64	6.8Ø	
HØ557-385	4UØ557-38	1.36 .16	2.26 .21		1	*	.Ø334 MP	2.175ØØ	1.62	2.7Ø	

H0630-541	2A0626-541 4U0627-54	1.98	.18	2.23	.13	SC0630-541	6	*	.0502	V	2.520	5.55	6.25	2
H0906-095	2A0906-095 4U0900-09	3.96	.28	4.16	.26	ABELL 754	6	*	.0537	C1	2.440	12.3	12.9	
H0917-074		1.36	.28	1.21	.3		7				2.500			
H0943-141	2A0943-140 4U0937-12	3.14	.25	3.97	.54	NGC2992	2	*	.0062	DV	2.175	.114	.143	
H0952+699	2A0954+700 1M0943+712 4U0954+70	1.32	.2	1.17	.2	M82	2	*	.0013	DV	2.480	.0024	.0021	
H1019+203	A1021+198	1.71	.24	.96	.3	NGC3227	2	*	.0033	W1	2.175	.0175	.0098	
H1034-273	2A1033-270 4U1033-26	2.19	.21	2.25	.3	ABELL 1060	6	*	.0114	M	2.880	.355	.365	
H1136-375	2A1135-373 4U1136-37	1.95	.23	<.6		NGC3783	1	*	.0091	W1	2.175	.152		
H1208+397	2A1207+397 1M1207+397 4U1206+39	6.34	.26	10.64	.36	NGC4151	1	*	.0033	W1	2.070	.0607	.104	
H1219+305	2A1219+305	1.61	.25	1.3	.3	1219+305	3	*			2.340			
H1226+023	2A1225+022 4U1226+02	3.46	.26	3.8	.37	3C273	5	*	.158	MS	2.040	81.6	89.6	
H1228+127	2A1228+125 1M1228+127 4U1228+12	14.2	.33	14.25	.33	VIRGO CL.	6	*	.0037	DV	2.850	.239	.240	
H1238-049	4U1240-05	1.71	.26	1.09	.41	NGC4593	1	*	.0085	DV	2.175	.116	.0741	
H1246-410	2A1246-410 1M1247-410 4U1246-41	5.15	.23	5.64	.37	CEN CL.	6	*	.0118	FO	2.740	.851	.932	
H1256-171		1.45	.28	<1.8		ABELL 1644	6	*	.0449	HSM	2.520	3.24		
H1257-042		1.47	.27	1.41	.53	ABELL 1651	6	**	.0826	HSM	2.520	11.3	10.9	
H1257+283	2A1257+283 1M1257+281 4U1257+28	14.67	.28	16.1	.32	ABELL 1656	6	*	.023	N	2.440	8.25	'9.05	
H1324-311	2A1326-311 1M1329-314 4U1325-31	2.83	.25	2.74	.45	SC1326-31	6	*	.073	L	2.520	17.0	16.4	3
H1325-020		1.47	.25	<1.0			7				2.500			
H1332-336	2S1333-34	2.12	.18	2.59	.35	MCG6-30-15	1	*	.006	W3	2.175	.0717	.0876	
H1344-333 ?	2A1344-325	3.23	.27	2.49	.37	SC1344-32	6	**	.0144	L	2.520	.732	.565	

H1347+268	2A1346+266 4U1348+25	2.36	.25	2.91	.4	ABELL 1795	6	*	.Ø621	H	2.52Ø	1Ø.2	12.6
H1346-3ØØ	2A1347-3ØØ	3.7	.21	3.43	.37	IC4329A	1	*	.Ø138	W1	2.175	.665	.616
H1411-Ø31	2A141Ø-Ø29 1M141Ø-Ø3Ø 4U141Ø-Ø3	2.69	.22	2.62	.43	NGC55Ø6	2	*	.ØØ56	DV	2.175	.Ø793	.Ø772
H1416+256	2A1415+255 4U1415+25	2.92	.23	2.77	.32	NGC5548	1	*	.Ø166	W1	2.175	.76Ø	.721
H15Ø8+Ø6Ø	2A15Ø8+Ø62 1M1514+Ø68	3.ØØ	.29	2.35	.36	ABELL 2Ø29	6	*	.Ø767	F	2.52Ø	19.9	15.6
H1513+Ø7Ø CONFUSED? WITH 2A1519+Ø82		1.51	.28	1.9	.36	ABELL 2Ø52	6	*	.Ø344	M	2.52Ø	1.97	2.48
H1521+282	2A1518+274 4U1521+28	1.25	.2	1.69	.33	ABELL 2Ø65	6	*	.Ø721	S	2.52Ø	7.3Ø	9.87
H1556+274	2A1556+274 4U1556+27	3.14	.24	2.87	.23	ABELL 2142	6	*	.Ø9Ø3	H	2.42Ø	27.9	25.5
H16ØØ+161	2A16ØØ+164 4U16Ø1+15	1.82	.23	2.	.41	ABELL 2147	6	*	.Ø377	N	2.74Ø	3.11	3.42
H1627+396	2A1626+396 4U1627+39	2.72	.18	2.82	.24	ABELL 2199	6	*	.Ø312	N	2.74Ø	3.17	3.29
H163Ø+Ø57	2A163Ø+Ø57 4U1636+Ø5	1.26	.24	<1.8			7				2.5ØØ		
H1652+398	4U1651+39	1.81	.18	1.71	.28	MKN5Ø1	3	*	.Ø34	DV	2.34Ø	2.14	2.Ø3
H17Ø7+788	2A17Ø5+786 1M17Ø6+785 4U17Ø7+78	2.53	.12	2.42	.1	ABELL 2256	6	*	.Ø6Ø3	F	2.48Ø	1Ø.1	9.68
H1829-591	4U183Ø-6Ø	1.55	.21	.71	.24		7				2.5ØØ		
H1834-653		1.36	.18	1.Ø8	.23	ESO1Ø3-G35	1	**	.Ø13	W3	2.175	.217	.172
H1846-786	1M1849-781 4U1916-79	1.33	.16	1.48	.21		7				2.5ØØ		
H1917-587	2A1914-589 4U1924-59	1.7Ø	.17	1.64	.26	ESO141-G55	1	*	.Ø368	W2	2.175	2.2Ø	2.12
H2ØØ9-569	2A2ØØ9-569	3.19	.21	3.Ø9	.25	SC2ØØ8-569	6	*	.Ø6	B2	2.52Ø	12.8	12.4
H2Ø41-1Ø9	2A2Ø4Ø-115	2.Ø8	.24	2.41	.31	MKN5Ø9	1	*	.Ø355	W1	2.175	2.5Ø	2.73
H2154-3Ø4	2A2151-316	4.3Ø	.24	2.33	.32	PKS2155-3Ø4	3	*	.17	CTB	2.525	146.	79.1

H2151-6Ø5	2A2155-6Ø9 1M214Ø-6Ø2 4U2126-6Ø	1.29	.21	1.35	.25	STR2159-6Ø2	6	**	.1ØØ8	WF	2.52Ø	14.9	15.6
H2158-321	2A2151-316	2.ØØ	.23	1.4	.29	NGC7172	4	**	.ØØ9	DV	2.57Ø	.18Ø	.126
H22Ø9-471		1.Ø7	.21	1.83	.28	NGC7213	1	*	.ØØ58	DV	2.175	.Ø338	.Ø578
H2216-Ø27	2A222Ø-Ø22	1.55	.24	.98	.29	3C445	2	**	.Ø562	OKP	2.175	4.71	2.98
H2233-261	2A2237-256	1.39	.22	1.94	.3	NGC7314	2	**	.ØØ56	DV	2.175	.Ø41Ø	.Ø572
H23Ø1+Ø86	2A2259+Ø85 4U23ØØ+Ø8	1.77	.25	1.45	.39	NGC7469	1	*	.Ø167	W1	2.175	.466	.382
H23Ø2-Ø9Ø	2A23Ø2-Ø88 4U23Ø5-Ø7	1.88	.25	2.3	.34	MCG2-58-22	1	*	.Ø479	W2	2.175	4.14	5.Ø6
H2316-426	2A2315-428	2.51	.23	3.Ø4	.29	NGC7582	2	*	.ØØ48	DV	2.175	.Ø543	.Ø658
H2342+Ø89	4U2344+Ø8	1.31	.27	.93	.33	ABELL2657	6	*	.Ø414	N	2.52Ø	2.49	1.77

COLUMN CAPTIONS:

(1) : H NAME

(2) : PREVIOUS NAMES

(3) : 1ST SCAN FLUX AND 1-SIGMA ERROR (R15 COUNTS/SEC)

(4) : 2ND SCAN FLUX AND 1-SIGMA ERROR (R15 COUNTS/SEC)

(5) : IDENTIFICATION

(6) : TYPE OF OBJECT:
1 = SEYFERT 1 GALAXY
2 = SEYFERT 2, NELG, N OR OTHER ACTIVE GALAXY
3 = BL LACERTE OBJECT
4 = NORMAL GALAXY
5 = QSO
6 = CLUSTER OF GALAXIES
7 = UNIDENTIFIED

(7) : QUALITY OF IDENTIFICATION: * = CERTAIN: SAS-3 OR HEAO-1 MODULATION COLLIMATOR POSITION OR EINSTEIN OBSERVATORY POSITION
** = POSSIBLE

(8) : REDSHIFT VALUE AND REFERENCE:
B = BAHCALL,N.A.,SARGENT,W.L.W.,1977,AP.J.,217,L19
B2 = BAHCALL,N.A.,AP.J.,217,L77
C1 = CORWIN,H.G.JR.,1971,PUBL.ASTRON.SOC.PACIFIC,83,32Ø
C2 = CORWIN,H.G.JR.,1974,A.J.,79,1356
CMR = CANIZARES,C.R.,MCCLINTOCK,J.E.,RICKER,G.R.,1978,AP.J.,226,L1
CTB = CHARLES,P.,THORSTENSEN,J.,BOWYER,S.,1979,NATURE,281,285
DV =DEVAUCOULEURS,DEVAUCOULEURS AND CORWIN SECOND REFERENCE CATALOG OF BRIGHT GALAXIES 1976
F = FABER,S.,DRESSLER,A.,1977,A.J.,82,167
FD = FOSBURY,R.A.E.,DISNEY,M.J.,1976,AP.J.,2Ø7,L75
FO = FORMAN,W.,JONES,C.,TANANBAUM,H.,1976,AP.J.,2Ø6,L29
H = HINTZEN,P.,SCOTT,J.S.,1979,AP.J.,232,L145

HSM = HINTZEN,P.SCOTT,J.S.,MCKEE,J.D. 1980 AP.J. IN PRESS
L = LUGGER,P.,1978,AP.J,221,745
M = MELNICK,J.,SARGENT,W.,1977,AP.J.,215,401
MA = MACCAGNI,D.,TARENGHI,M.,COOKE,B.A.,MACCACARO,T.,PYE,J.P.,RICKETTS,M.J.,CHINCARINI,G.,1978,ASTRON.&ASTROPHYS.,62,127
MQ = MELNICK,J.,QUINTANA,H.,1975,AP.J.,198,L97
MP = MCHARDY,J. AND PYE,J IAU CIRCULAR 3587 1981
MS = SCHMIDT,M.,1968,AP.J.,151,393
N = NOONAN,T.,1973,A.J.,78,26
OKP = OSTERBROK,D.E.,KOSKI,A.T.,PHILLIPS,M.M.,1976,AP.J.,206,898
S = SPINRAD,H.,1977,PUB.A.S.P.,89,116
SC = SCHWARTZ,D.,SCHWARZ,J,TUCKER,W.,,1980,AP.JLETT. 238,L59
V = VIDAL,N.V.,1975,PUBL.ASTRON.SOC.PACIFIC,87,625
W1 = WEEDMAN,D.W.,1977,ANN.REV.ASTRON.ASTROPHYS.,15,69
W2 = WEEDMAN,D.W.,1978,MON.NOT.R.ASTR.SOC.,184,11P
W3 = WEEDMAN,D.W.,1979,PROC.IAU GENERAL ASSEMBLY,MONTREAL
WF = WEST,R.M.,FRANDSEN,S.,1980,ESO SCIENT. PREPRINT N.110,

(9) : CONVERSION FACTOR (1.E-11 ERGS/CM2 SEC PER R15 COUNTS/SEC)

(10) : 1ST SCAN LUMINOSITY (1.E44 ERGS/SEC)

(11) : 2ND SCAN LUMINOSITY (1.E44 ERGS/SEC)

(12) : NOTES
1.IPC DETECTION BUT NOT IDENTIFIED AT PRESENT
2.MULTIPLE CLUSTER FORMAN ET AL 1981
3.MULTIPLE CLUSTERS PERRENOD AND HENRY 1981

TABLE 2

HIGH LATITUDE (B> 2Ø DEG) X-RAY SOURCES EXCLUDED FROM LOG N-LOG S ANALYSIS

/
/

2AØØ39+41	1.95	.22	1.47	.37	GALAXY(M31)	V1
HØ123+Ø75	1.62	.26	.73	.29	TRANSIENT(HD8357)	M1,G2
2AØ311-22	2.64	.22	2.23	.28	STAR	G1
HØ328+Ø5	<.85		2.92	.27	STAR	D1
4UØ336+Ø1	1.27	.24	1.41	.26	STAR (HR1Ø99)	W1
2SØ512-39	6.56	.21	5.64	.25	GLOB CLUSTER(NGC1851)	B1
2AØ526-32	1.99	.16	2.55	.2Ø	STAR	C1
HØ751+22	1.36	.21	<.6		STAR(U GEM)	S3
2A1Ø52+6Ø	1.34	.21	<.8		STAR(BD 61+1211)	S1
2A1249-28	4.41	.28	5.51	.33	STAR (EX HYA)	S1
3U1616-15	>5ØØ.		>5ØØ.		SCØX-1(V818 SCO)	B1
3U1655+35	8Ø.8	.43	3.47	.2Ø	HER X-1(HZ HER)	B1
2A17Ø4+24	<.8		2.46	.21	STAR	G4
2A1815+5Ø	4.11	.12	3.98	.14	STAR(AM HER)	S4
H2215-Ø8	1.5Ø	.23	1.2Ø	.4Ø	STAR(WOLF 1561??)	T1,S2
4U2127+14	5.32	.22	4.97	.35	GLOB CLUSTER(NGC 7Ø78)	B1
H2252-Ø35	2.36	.25	2.43	.2Ø	STAR	G3

/
/

SOURCES IN AND NEAR THE LMC AND SMC HAVE BEEN OMITTED FROM THIS TABLE AND FROM TABLE 1.THE EXPERIMENT HAS DETECTED FLUX FROM SMX X-1,2,3 LMC X-1,2,3,4,5 AND THE LMC TRANSIENT SOURCE Ø535-668

/
/

REFERENCES:

B1=BRADT,DOXSEY,JERNIGAN 1979
C1=CHRALES,THORSTENSEN,BOWYER,MIDDLEDITCH 1979
D1=DOXSEY,MCCLINTOCK,PETRO,REMILLARD,SCHWARTZ
G1=GRIFFITHS,WARD,BLADES,WILSON 1979
G2=GARCIA,BALIUNAS,CONROY,JOHNSTON,RALPH,ROBERTS,SCHWARTZ,TONRY 198Ø
G3=GRIFFITHS,LAMB,WARD,WILSON,CHARLES,THROSTENSEN,MCHARDY,LAWRENCE 198Ø
G4=GARCIA,CONROY,DOXSEY,GRIFFITHS,JOHNSTON,RALPH,ROBERTS,SCHWARTZ 198Ø
M1=MARSHALL,BOLDT,MUSHOTZKY,PRAVDO,ROTHSCHILD,SERLEMITSOS 1979
S1=SCHWARTZ,BRADT,BRIEL,DOXSEY,FABBIANO,GRIFFITHS,JOHNSTON,MARGON 1979
S2=SCHWARTZ 198Ø (PRIVATE COMMUNICATION)
S3=SWANK,BOLDT,HOLT,ROTHSCHILD,SERLEMITSOS 1978
S4=SWANK,LAMPTON,BOLDT,SERLEMITSOS 1977
T1=TSIKOUDI,SWANK 198Ø
V1=VAN SPEYBROECK,EPSTEIN,FORMAN,GIACCONI,JONES,LILLER,SMARR 1979
W1=WHITE,SANFORD,WEILER 1978

REFERENCES

Avni, Y., Bahcall, J.N. 1980, Ap. J. 235, 694.

Bahcall, N. 1979, Ap. J. 232, 639.

Birnbaum, Z.W., Tingey, F.M. 1951, Ann. Math. Stat 22, 592.

Boldt, E. 1980, Invited Talk at AAS Meeting, NASA TM 80659.

Bradt, H., Doxsey, R.E., and Jernigan, J.G. 1979, Advances in Space Exploration.

Charles, P. Thorstensen, J., Bowyer, S., and Middleditch, J.1979, Ap. J. (Letters) 231, L131.

Crawford, D.E., Jauncy, D.L., Murdoch, H.S. 1970, Ap. J. 162, 405.

DeVaucouleurs, G. 1958, A.J. 63, 253.

DeVaucouleurs, G., DeVaucouleurs, A. and Corwin, H. 1976, Second Reference Catalog of Bright Galaxies, Univ. of Texas Press.

DeZotti, G. 1980, preprint.

Doxsey, R., McClintock, J., Petro, L., Remillard, R., and Schwartz, D. 1981 B.A.A.S. 13, 558.

Elvis, M., Maccacaro, T., Wilson, A., Ward, M., Penston, M., Fosbury, R., Perola, G. 1978, MNRAS 183, 129.

Fabian, A.C. and Rees, M.J. 1978, MNRAS 185, 109.

Forman, W., Bechtold, J., Blair, W., Giacconi, R., Van Speybroeck, L, and Jones, C. 1981, Ap. J. (Letters) 243, L133.

Garcia, M., Baliunas, S.L., Conroy, M., Johnston, M.D., Ralph, E., Roberts, W., Schwartz, D.A., and Tonry, J. 1980, Ap. J. (Letters) 240, L107.

Garcia, M., Conroy, M., Doxsey, R., Griffiths, R.E., Johnston, M., Ralph, E., Roberts,W., and Schwartz, D.A. 1980, BAAS 12, 527.

Giacconi, R., Bechtold, J., Branduaradi, G., Forman, W., Henry, J.P., Jones, C., Kellogg, E., van der Laan, H., Liller, W., Marshall, H., Murray, S.S., Pye, J., Schreier, E., Sargent, W.G.W., Seward, F., and Tananbaum, H. 1979, Ap. J. (Letters) 234, L1.

Griffiths, R.E., Ward, M.J., Blades, J.C., Wilson, A.S. 1979, Ap. J. 232, L27.

Griffiths, R.E., Lamb, D.Q., Ward, M.J., Wilson, A.J., Charles, P.A., Thorstensen, J., McHardy, I.M. and Lawrence, A. 1980, MNRAS 193, 25p.

Holt, S.S. 1980, invited talk at Cambridge HEAD meeting, NASA TM 82010.

Huchra, J.P. and Sargent, W.L.W. 1973, Ap. J. 186, 433.

Huchra, J.P. 1977, Ap. J. Suppl. 35, 171.

Huchra, J.P. 1980, private communication.

Kriss, G.A., Canizares, C.R., and Ricker, G.R. 1980, Ap. J. 242, 492.

Lightman, A., Hertz, P., and Grindlay, J.E. 1980, Ap. J. 241, 367.

Marshall, F.E., Boldt, E.A., Holt, S.S., Mushotzky, R.F., Pravdo, S.H., Rothschild, R.E., and Serlemitsos, P.J. 1979, Ap. J. (Suppl) 40, 657.

Marshall, F.E., Boldt, E.A., Holt, S.S., Miller, R., Mushotzky, R.F., Rose, L.A., Rothschild, R., and Serlemitsos, P.J. 1980, Ap. J. 235, 4.

McHardy, I. 1978, MNRAS 182, 760.

McKee, J., Mushotzky, R., Boldt, E., Holt, S., Marshall, F.E., Pravdo, S., and Serlemitsos, P. 1980, Ap. J. 242, 843.

Murdoch, H.S., Crawford, D.F., and Jauncey, D.L. 1973, Ap. J. 183, 1.

Mushotzky, R.F. 1979, Proceedings of the Erice Symposium on X-Ray Astronomy, eds. R. Giacconi and G. Setti, p. 171.

Mushotzky, R., Marshall, F.E., Boldt, E., Holt, S., and Serlemitsos, P. 1980, Ap. J. 235, 36.

Perrenod, S. and Henry, J.P. 1981, preprint.

Pye, J.P. and Warwick, R.S. 1979, MNRAS 187, 905.

Rothschild, R., Boldt, E., Holt, S., Serlemitsos, P., Garmire, G., Agrawal, P., Riegler, G., Bowyer, S., and Lampton, M. 1979, Space Science

Instrumentation 4, 265.

Schwartz, D.A. 1978, Ap. J. 222, 8.

Schwartz, D.A., Bradt, H., Briel, V., Doxsey,R.E., Fabbiano, G., Griffiths, R.E., Johnston, M.D., Margon, B. 1979, Ap. J. 84, 1560.

Schwartz, D.A., 1979 in (COSPAR) X-Ray Astronomy, W.A. Baity and L.E. Peterson (eds), Pergamon Press, Oxford and New York, p.453.

Schwartz, D.A. 1980, private communication.

Swank, J., Boldt, E.A., Holt, S.S., Rothschild, R.E., and Serlemitsos, P.J. 1978, Ap. J. (Letters) 226, L133.

Swank, J., Lampton, M., Boldt, E., Holt, S., and Serlemitsos, P. 1977, Ap. J. (Letters) 216, L71.

Tananbaum, H., Peters, G., Forman, W., Giacconi, R., Jones, C., and Avni, Y. 1978, Ap. J. 223, 74.

Tsikoudi, V. and Swank, J. 1981, in preparation.

Van Speybroeck, L, Epstein, A., Forman, W., Giacconi, R., Jones, C., Liller, W., and Smarr, L. 1979, Ap. J. 234, L45.

Warwick, R.S. and Pye, J.P. 1978, MNRAS 183, 169.

Weedman, D. 1979, Invited Talk at Montreal IAU General Assembly.

Weinberg, S. 1972, Gravitation and Cosmology

West, R.M., and Frandsen, S. 1980, ESO Scientific Preprint, No. 110.

White, N.E., Sanford, P.W., and Weiler, E.J. 1978, Nature 274, 569.

Worrall, D., Boldt, E., Holt,S., Mushotzky, R., and Serlemitsos, P. 1981, Ap. J. 243, 53.

FIGURE CAPTIONS

Figure 1. The completeness level of the present survey vs ecliptic latitude. The diamonds are for the first pass and the crosses for the second pass. The lower histogram is the sky fraction in each ecliptic latitude bin (right hand scale). The centre of the diamonds and crosses is 5 times the mean error for a source located in that ecliptic latitude bin and the size of the error bar is the standard deviation of this error. Since we truncate at 1.25 R15 counts all of our sources at ecliptic latitude greater than 30° lie well above the 5σ level. We estimate that residual incompleteness of sources at levels less than 1.4 cts is less than 3 sources and zero sources greater than this limit.

Figure 2. The error boxes for H0328+025 and H0917-074. The inner and outer boxes are the 90% confidence boxes as described in Marshall et al. 1979. The inner box assumes that the source was roughly constant during our period of observation.

Figure 3. The distribution of the non-galactic sources detected in this survey in supergalactic coordinates.

Figure 4. The probability distributions for κ and α. The top panel shows the AML probability vs. α in the first pass data, the middle panel shows the AML probability vs. α in the second pass. The bottom panel shows the 68 and 95% joint probability contour for κ and α for the first pass data. The + marks the best fit.

Figure 5. The differential log N - log S distribution for our sample. The best fit is indicated. The highest flux point is indicated by a dashed cross because its upper flux bound is not well defined. (1st pass data)

Figure 6. The AML Kolomogorov-Smirnov test distribution for an $\alpha = 2.5$ model. The 50 and 95% probability bounds are indicated. (1st pass data)

Figure 7. The ratio of the number of observed sources N_{obs} to the number of expected sources for $\alpha = 2.5$ log N - log S law. (1st pass data)

Figure 8a. The cluster of galaxies differential luminosity function for the first pass data.

8b. The same information for the second pass data. The best fit power law models are indicated on both panels.

Figure 9. the AML probability vs. γ the slope of the power law differential luminosity function for clusters of galaxies for the first and second passes including and excluding the Virgo cluster.

Figure 10. Same as Figure 9 but for the exponential luminosity function..

Figure 11. The Seyfert galaxy luminosity function for the first pass data. The best fit power law differential model is indicated. The insert shows the AML probability vs. γ the slope of the luminosity function.

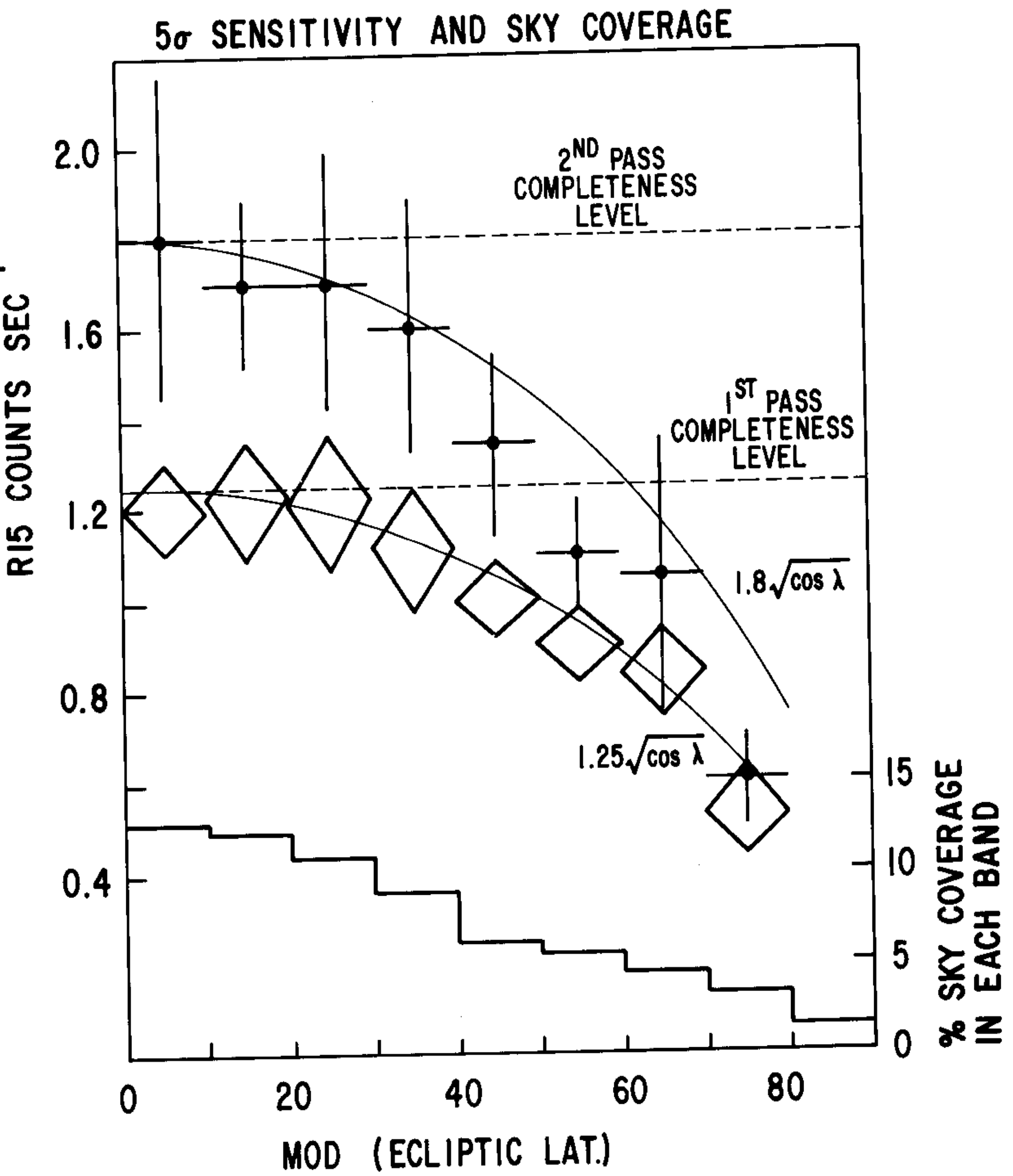

5σ SENSITIVITY AND SKY COVERAGE
2ND PASS
COMPLETENESS
LEVEL
1ST PASS
COMPLETENESS
LEVEL
1.8√cos λ
1.25√cos λ
R15 COUNTS SEC⁻¹
2.0
1.6
1.2
0.8
0.4
15
10
5
0
% SKY COVERAGE
IN EACH BAND
0
20
40
60
80
MOD (ECLIPTIC LAT.)

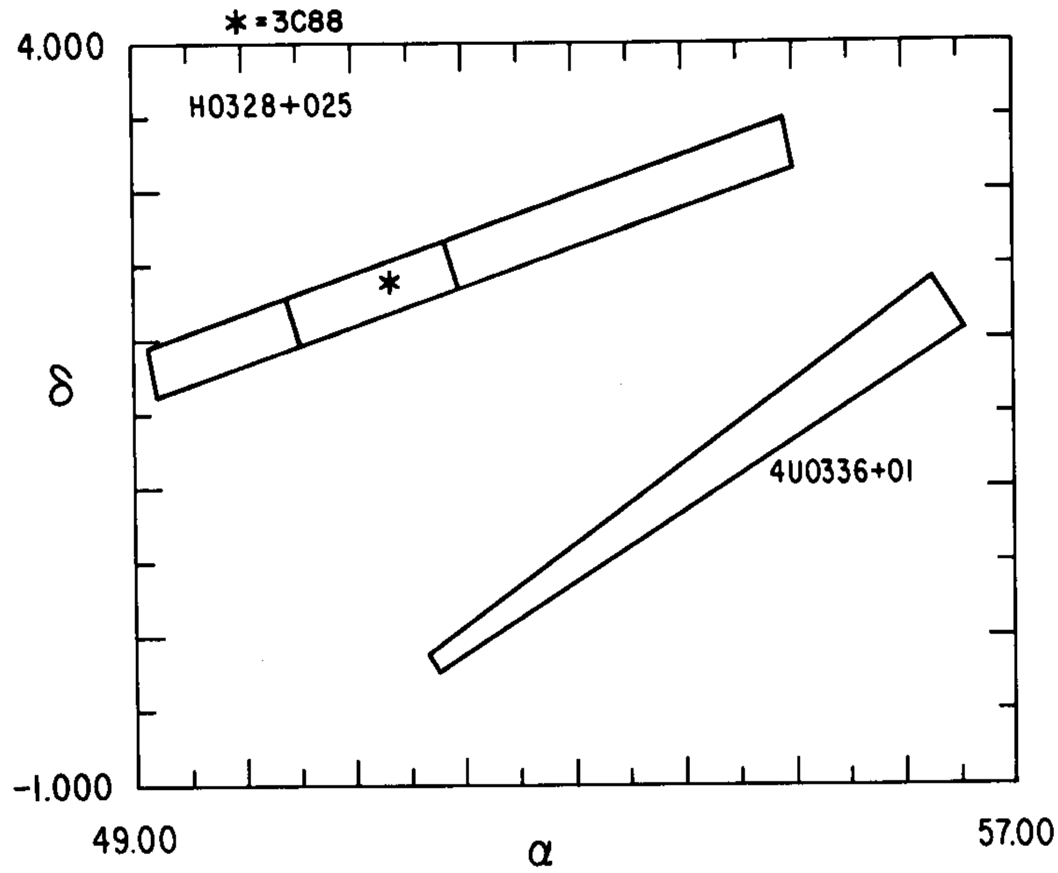

* = 3C88
4.000
H0328+025
4U0336+01
δ
-1.000
49.00
57.00
α

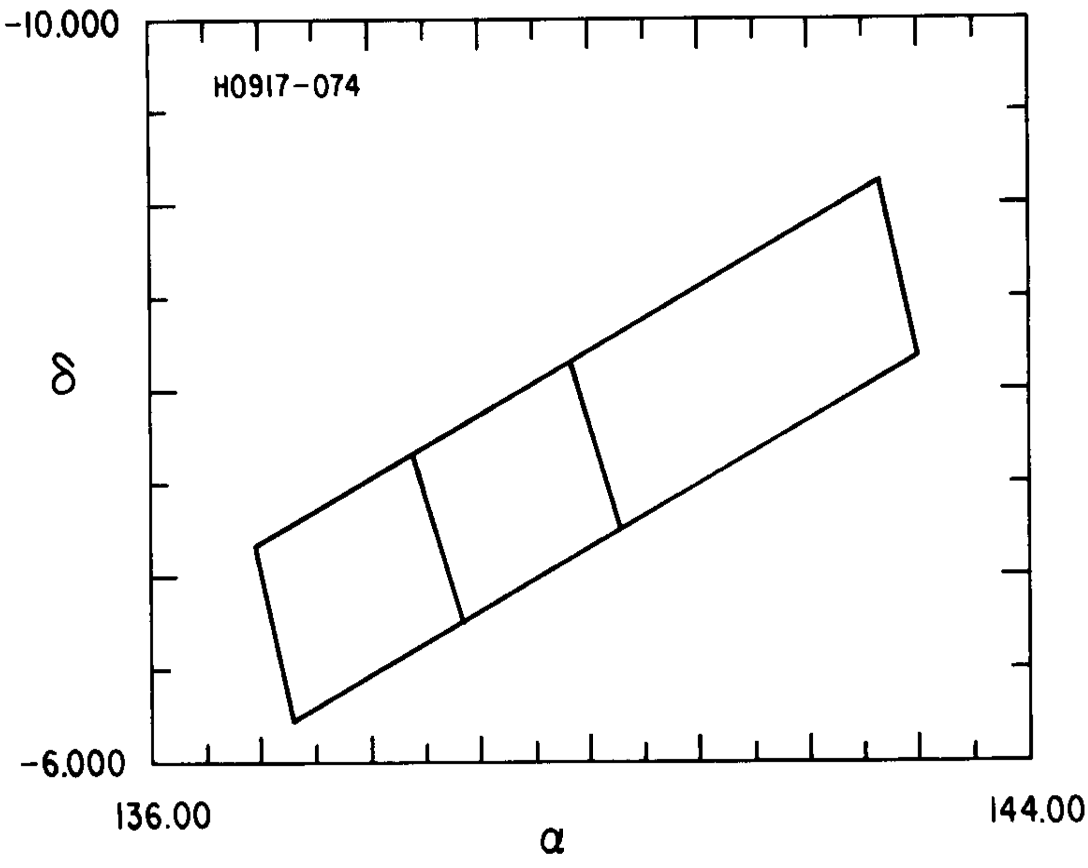

-10.000
H0917-074
δ
-6.000
136.00
144.00
α

SUPERGALACTIC COORDINATES

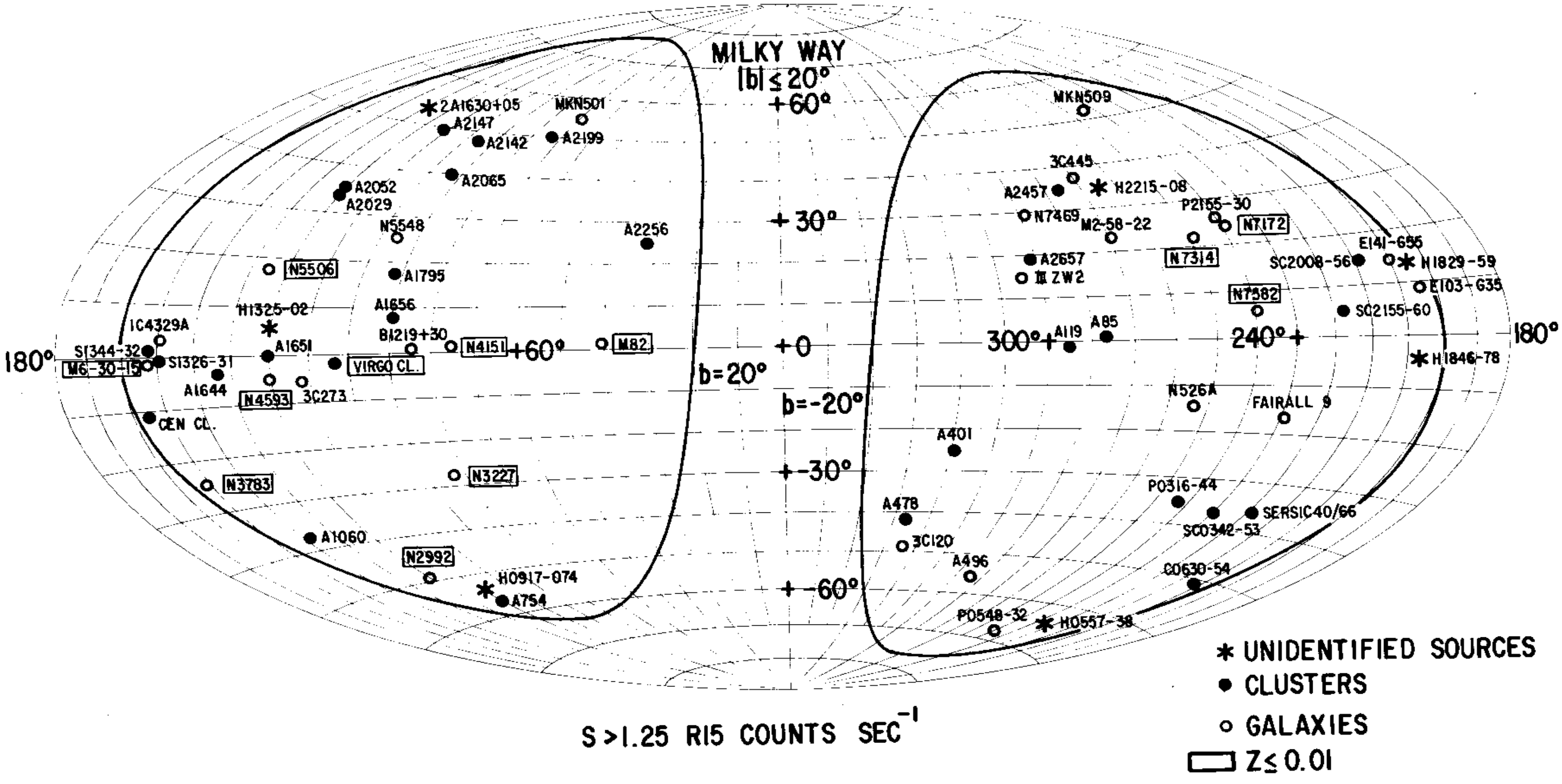

S >1.25 RI5 COUNTS SEC^{-1}

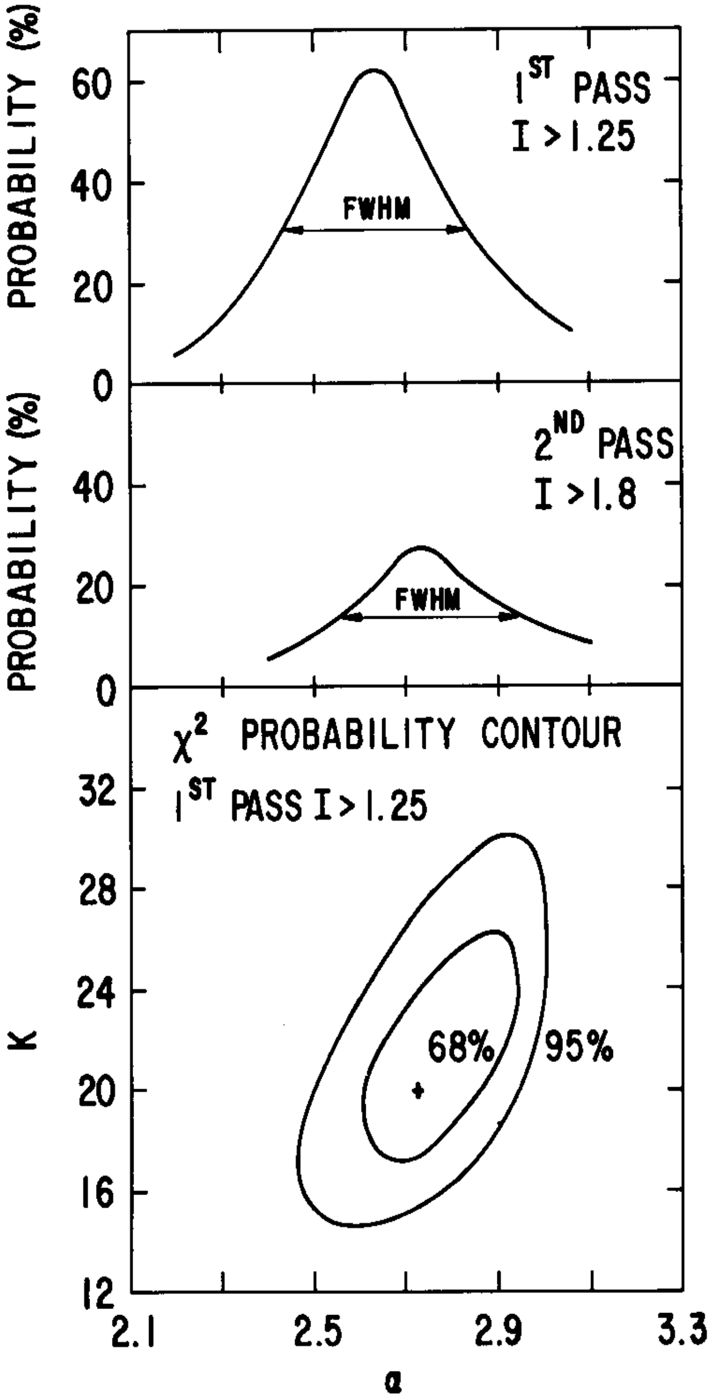
PROBABILITY (%)
60
40
20
0
1^{ST} PASS
I > 1.25
FWHM
PROBABILITY (%)
40
20
0
2^{ND} PASS
I > 1.8
FWHM
χ^2 PROBABILITY CONTOUR
1^{ST} PASS I > 1.25
K
32
28
24
20
16
12
68%
95%
2.1
2.5
2.9
3.3
α

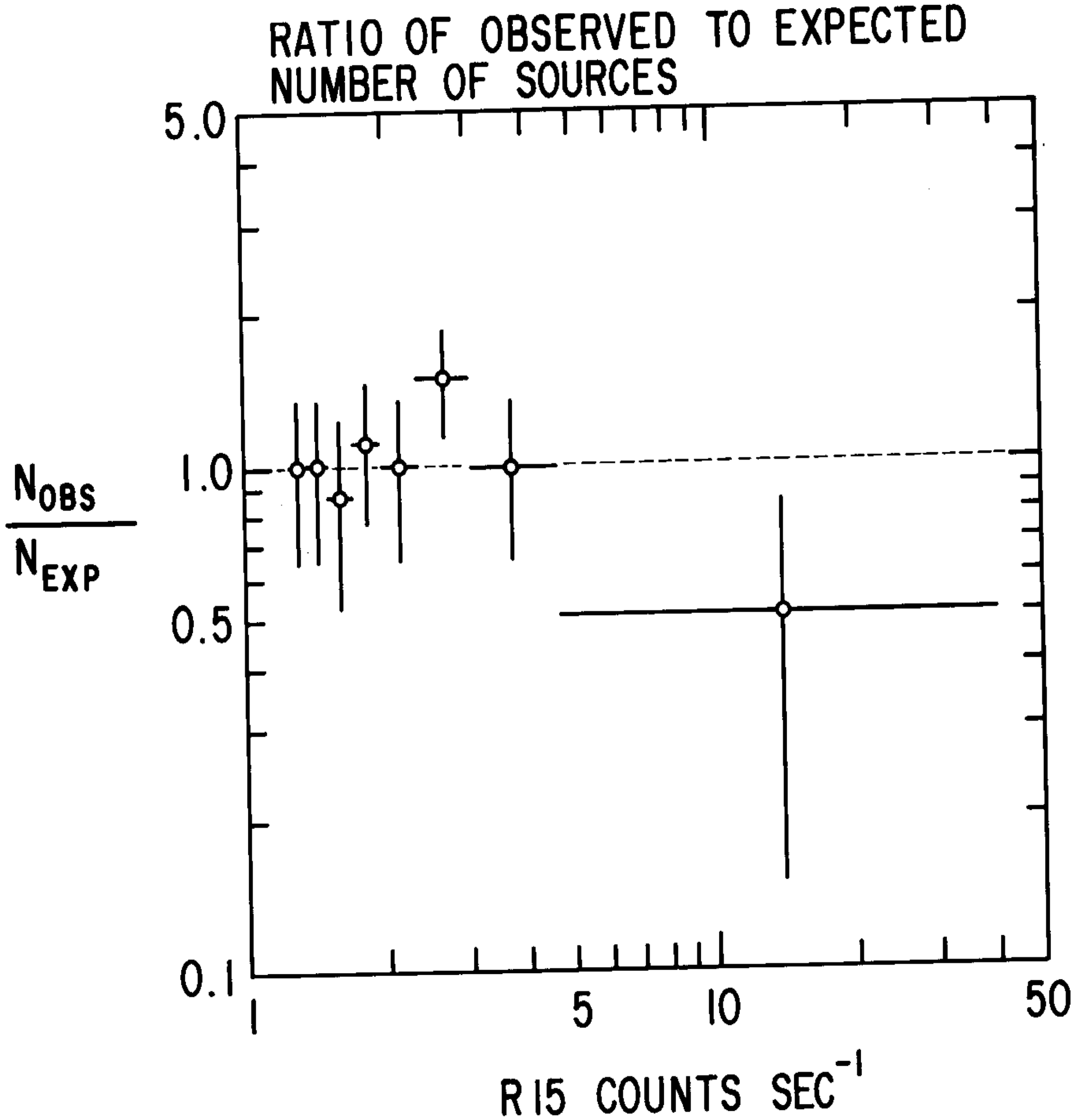

RATIO OF OBSERVED TO EXPECTED NUMBER OF SOURCES
5.0
1.0
0.5
0.1
$\frac{N_{OBS}}{N_{EXP}}$
1
5
10
50
R15 COUNTS SEC^{-1}

AML - KS TEST FOR EUCLIDEAN MODEL:
α=2.5 (1ST PASS - S ≥ 1.25 R15 COUNTS SEC^{-1})

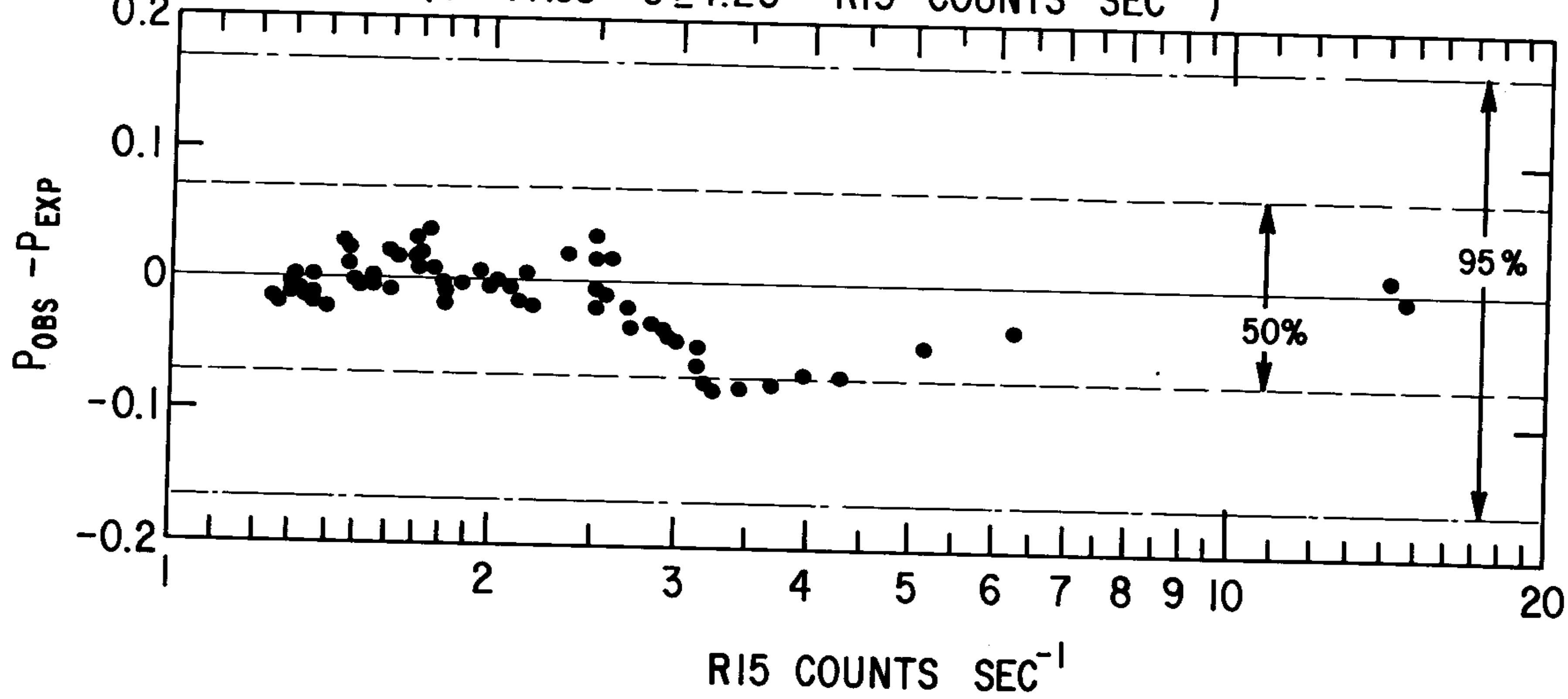

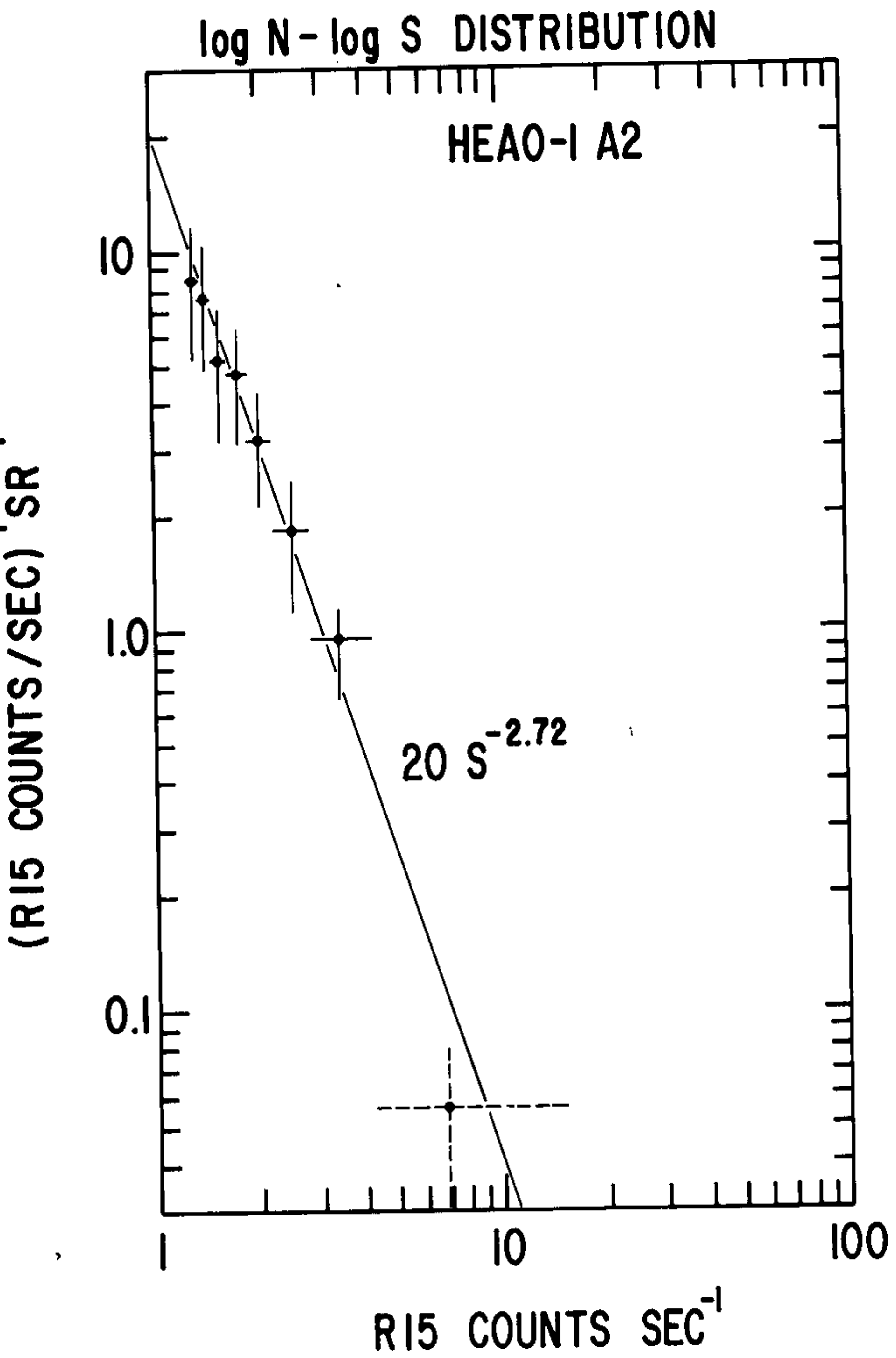
log N - log S DISTRIBUTION
HEAO-1 A2
20 S^-2.72
(R15 COUNTS/SEC)^-1 SR^-1
10
1.0
0.1
1
10
100
R15 COUNTS SEC^-1

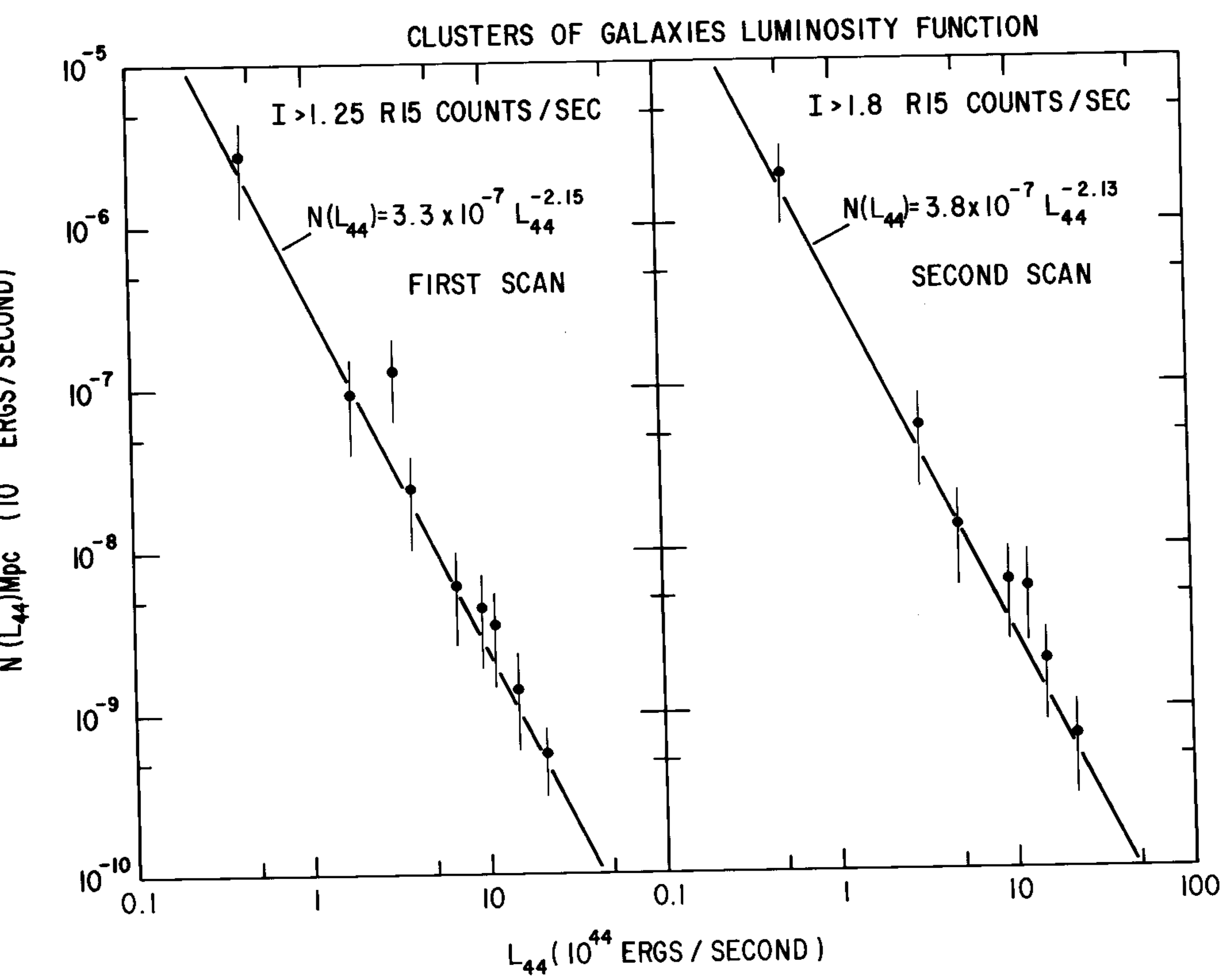
CLUSTERS OF GALAXIES LUMINOSITY FUNCTION
I > 1.25 R15 COUNTS / SEC
$N(L_{44}) = 3.3 \times 10^{-7} L_{44}^{-2.15}$
FIRST SCAN
I > 1.8 R15 COUNTS / SEC
$N(L_{44}) = 3.8 \times 10^{-7} L_{44}^{-2.13}$
SECOND SCAN
$N(L_{44}) Mpc^{-3} (10^{44}$ ERGS / SECOND$)^{-1}$
10^{-5}
10^{-6}
10^{-7}
10^{-8}
10^{-9}
10^{-10}
0.1
1
10
100
L_{44} (10^{44} ERGS / SECOND)

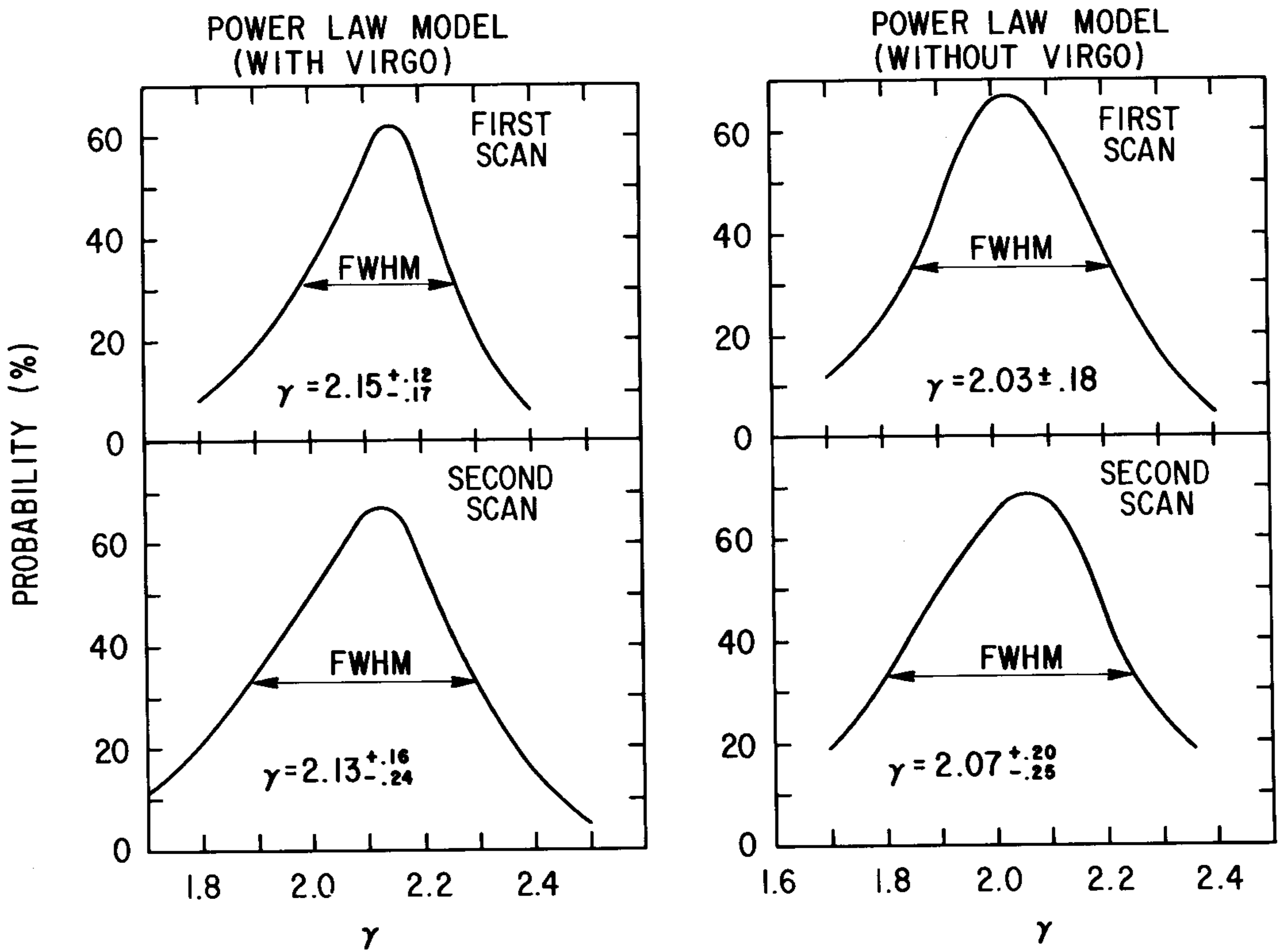
POWER LAW MODEL
(WITH VIRGO)
POWER LAW MODEL
(WITHOUT VIRGO)
FIRST SCAN
SECOND SCAN
FWHM
$\gamma = 2.15^{+.12}_{-.17}$
$\gamma = 2.13^{+.16}_{-.24}$
$\gamma = 2.03 \pm .18$
$\gamma = 2.07^{+.20}_{-.25}$
PROBABILITY (%)
γ
0
20
40
60
1.6
1.8
2.0
2.2
2.4

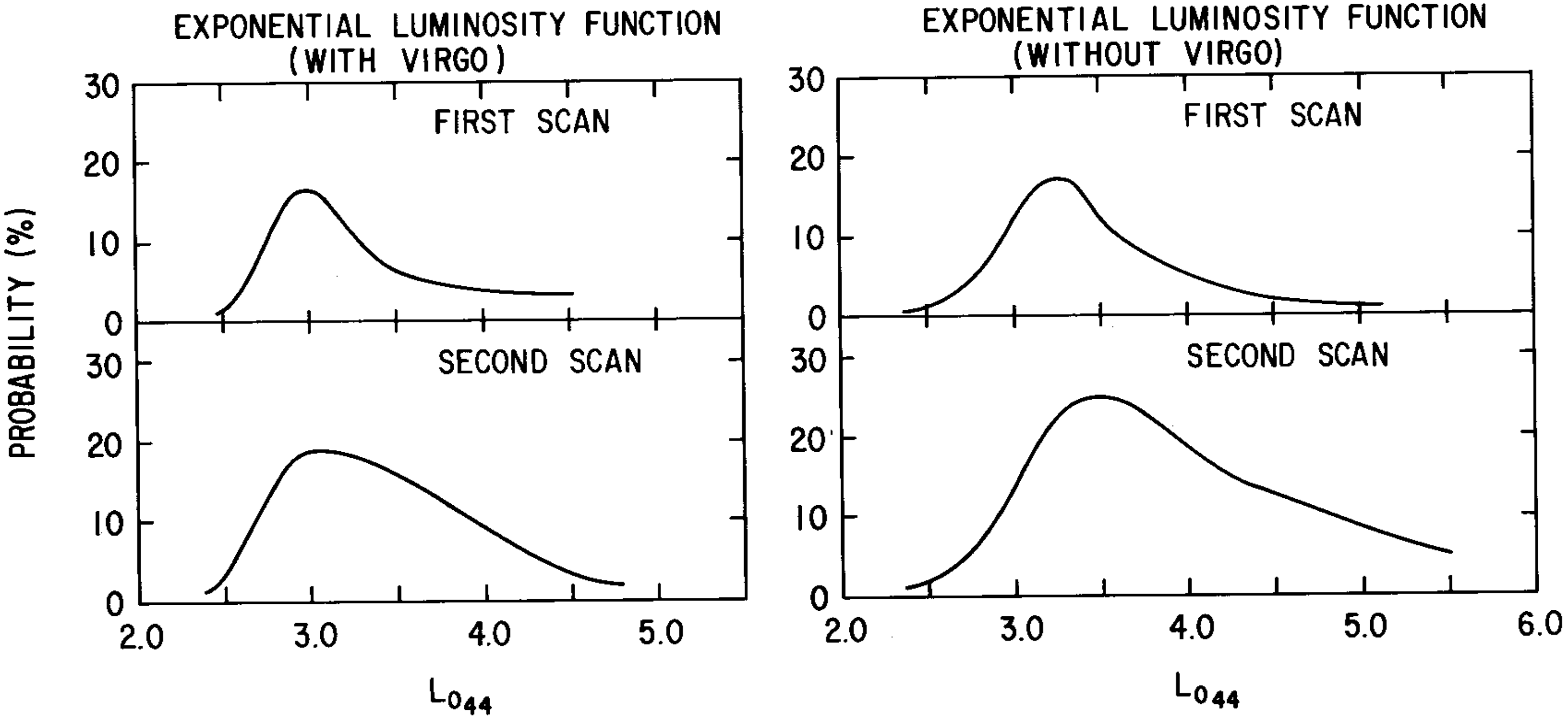
EXPONENTIAL LUMINOSITY FUNCTION
(WITH VIRGO)
FIRST SCAN
SECOND SCAN
PROBABILITY (%)
30
20
10
0
2.0
3.0
4.0
5.0
L044
EXPONENTIAL LUMINOSITY FUNCTION
(WITHOUT VIRGO)
FIRST SCAN
SECOND SCAN
6.0

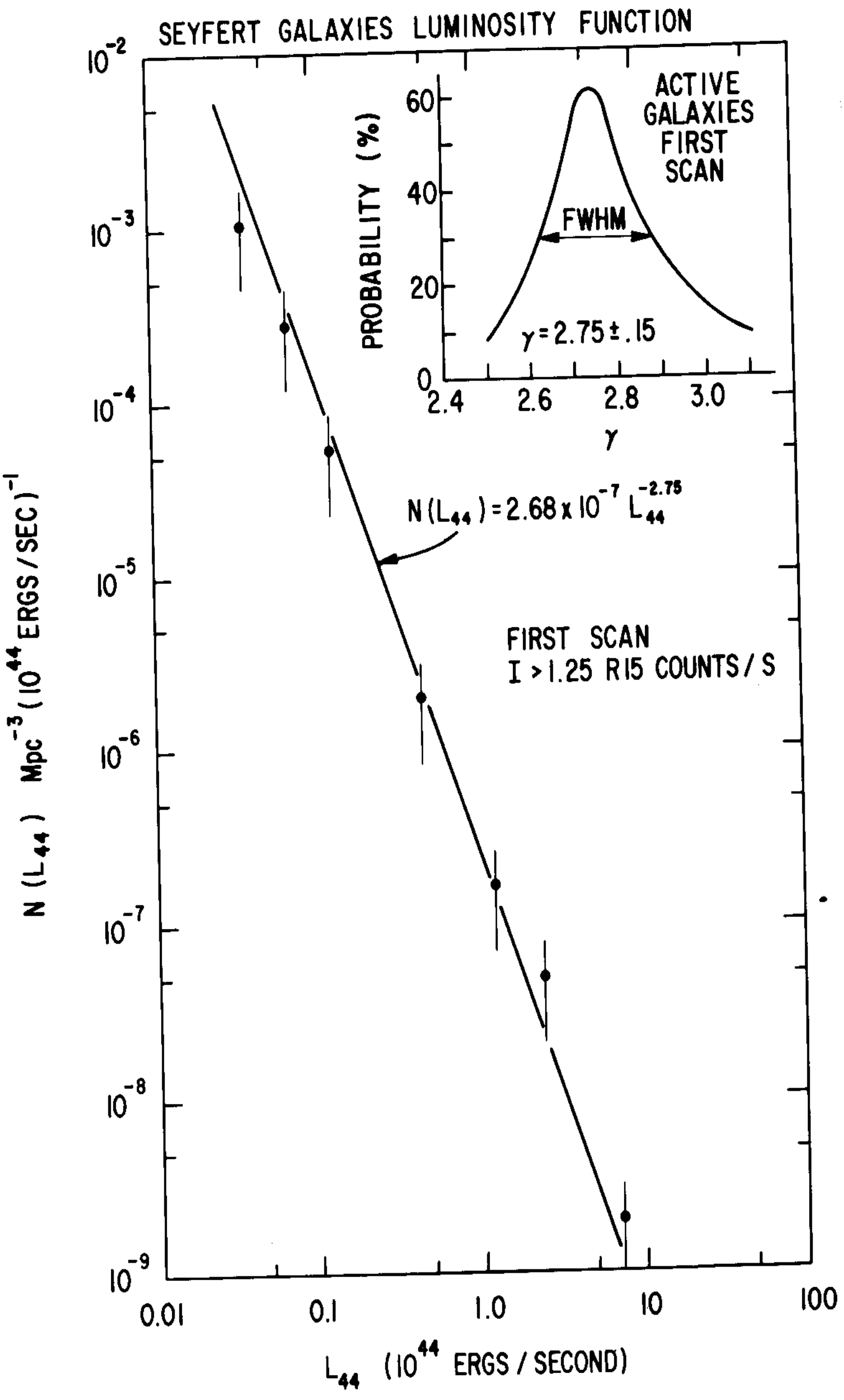

SEYFERT GALAXIES LUMINOSITY FUNCTION
ACTIVE GALAXIES FIRST SCAN
PROBABILITY (%)
FWHM
$\gamma = 2.75 \pm .15$
γ
$N(L_{44}) = 2.68 \times 10^{-7} L_{44}^{-2.75}$
FIRST SCAN
I > 1.25 R15 COUNTS / S
$N(L_{44})$ Mpc^{-3} $(10^{44}$ ERGS / SEC$)^{-1}$
L_{44} $(10^{44}$ ERGS / SECOND)

BIBLIOGRAPHIC DATA SHEET

1. Report No.: TM 82168
2. Government Accession No.:
3. Recipient's Catalog No.:

4. Title and Subtitle:
A Complete X-Ray Sample of the High Latitude ($|b| > 20^{o}$) Sky from HEAO-1 A-2: Log N - Log S and Luminosity Functions

5. Report Date: August 1981
6. Performing Organization Code: 661

7. Author(s): G. Piccinotti, R. Mushotzky, E. Boldt, S. Holt, F. Marshall, P. Serlemitsos, R. Shafer

8. Performing Organization Report No.:

9. Performing Organization Name and Address:
Code 661
Cosmic Radiations Branch
Laboratory for High Energy Astrophysics
NASA/Goddard Space Flight Center
Greenbelt, Maryland 20771

10. Work Unit No.:
11. Contract or Grant No.:
12. Sponsoring Agency Name and Address:
13. Type of Report and Period Covered:
14. Sponsoring Agency Code:

15. Supplementary Notes:
Accepted for publication in The Astrophysical Journal

16. Abstract

The HEAO-1 experiment A-2 has performed a complete X-ray survey of the 8.2 steradians of the sky at $|b| > 20^{0}$ down to a limiting sensitivity of $< 3.1 \times 10^{-11}$ ergs/cm^2 sec in the 2-10 keV band. Of the 85 detected sources (excluding the LMC and SMC sources) 17 have been identified with galactic objects, 61 have been identified with extragalactic objects and 7 remain unidentified. The log N - log S relation for the non-galactic objects is well fit by the Euclidean relationship. We have used the X-ray spectra of these objects to construct log N - log S in physical units. The complete sample of identified sources has been used to construct X-ray luminosity functions, using the absolute maximum likelihood method, for clusters of galaxies and active galactic nuclei.

17. Key Words (Selected by Author(s)):
X-Ray Sources, Luminosity Function, Cosmic X-Ray Background

18. Distribution Statement:

19. Security Classif. (of this report)	20. Security Classif. (of this page)	21. No. of Pages	22. Price*
U	U	48	

*For sale by the National Technical Information Service, Springfield, Virginia 22151.

GSFC 25-44 (10/77)

D- 46893
9/5/77 - 9/11/78

Time Span is not found on the tape it is in the documentation.

```
$NOP
$NOP ********** DOUT-1 ********
$EXEC TPLIST BS

INPUT PARAMETERS ARE:   AS FL=5=5 1

 TAPE NO.    1                 FILE NO.    1
 RECORD    1                   LENGTH    2400
              T A B L E   1

                                                                       (1)
        (2)          (3)           (4)          (5)    (6)(7)     (8)      (9)       (10)          (11
)
                         ------------------------------------------------------------
------------------------------------------------- H0008+105     2S0007+107     1.64  .21     <1.35
      IIIZW2       1   *   .0898 W3   2.175      12.9            ------------------------
------------------------------------------------------------------------------------ H0039-0
96     2A0039-096      2.64  .24       3.21  .38   ABELL 85     6   *    .0499 HSM   2.500       7 .25
   8.82      4U0037-10
                               ----------------------------------------------------
------------------------------------------------------ H0054-015     2A0054-015     1.74  .33
 2.13  .35    ABELL 119    6   *    .0446 N    2.550       3.89       4.76      4U0050-01
                                                                                          ---
------------------------------------------------------------------------------------------
------------------   H0111-149            1.49  .22         .93  .35              7              2.
500                                1      ----------------------------------------------------
------------------------------------------------------------ H0122-591     2A0120-591     1.29  .1
8       1.38  .2    FAIRALL9    1   *    .0461 W3   2.175      2.63        2.81      4U0106-59

  ------------------------------------------------------------------------------------------
----------------------

 TAPE NO.    1                 FILE NO.    1
 RECORD    2                   LENGTH    2400
 H0123-352     2A0120-353     2.52  .19      1.04  .28    NGC526A     1   *    .018  W3    2.175
.772        .319      4U0115-36
                                       ----------------------------------------------------
------------------------------------------------------------ H0206-019     H0206-019      1.34
.23       .87  .41    MKN590      1   *    .027  W1    2.175      0.91        0.59     ----------------
-----------------------------------------------------------------------------------------------
------   H0235-52       2A0235-52       2.12  .14        .99  .23               7
                          ------------------------------------------------------------
------------------------------------------------- H0256+134     2A0255+132     2.95  .24       3.03
 .33   ABELL 401    6   *    .0748 H     2.480      18.3       18.8      1M0254+132
                                                                                        4U0254+
13
                ---------------------------------------------------------------------------
---------------------------------------- H0316-443     2A0316-443     1.82  .19      1.07  .23   PKS0316-
443 6   **   .09    MA    2.520       16.7        9.82        4U0321-45
                                                                        ------------------
-----------------------------------------------------------------------------------------------  H
0335+096      2A0335+096      1.14  .22       1.86  .35    0335+096    6   *    .04    SC    2.810         2.2
5         3.67          4U0344+11
                                        ------------------------------------------------
------------------------------------------------------------ H0342-538     2A0343-536     1.4    .1
6       1.42  .17   CA0342-538  6   *    .052  MQ   2.520       4.21        4.27      1M0328-524

     4U0339-54

 TAPE NO.    1                 FILE NO.    1
 RECORD    3                   LENGTH    2400
---------------------------------------------------------------------------------------------------
---------------------    H0411+104     2A0411+103     2.61  .3        2.66  .34   ABELL 478    6   *   .
```

```
09   B   2.480   23.6   24.0   1M0405+100
                                                              4U0410+10
                                                                ----------------
-------------------------------------------------------------------------------------------------------
------ H0430-616   2A0430-615   2.53  .11   2.88  .14   SERSIC40/6  6  *  .0601 V   2.480
   10.1   11.4   1M0426-635
                                           4U0427-61
                                                             -------------------
----------------------------------------------------------------------------------------- H0431-1
34   2A0431-136   2.16  .29   1.73  .3   ABELL 496   6  *  .036  C2   2.520   3.09
  2.48   4U0431-12
                         ---------------------------------------------------------------
----------------------------------------------------- H0430+053   2S0430+05   2.04  .25
 1.53  .36   3C120   1  *  .033  DV   2.175   2.12   1.59   4U0432+05
                                                                                   ---
-------------------------------------------------------------------------------------------------------
----------------- H0548-322   1M0545-322   1.7   .18   1.2   .25   PKS0548-322  3  *  .069
  FD   2.675   9.64   6.80   4U0543-31
                                                  -----------------------------------
-------------------------------------------------------------------------- H0557-385   4U
0557-38   1.36  .16   2.26  .21   1  *  .0334 MP   2.17500   1.62   2.70
  ------------------------------------------------------------------------------------
----------------------

 TAPE NO.  1            FILE NO.  1
 RECORD  4              LENGTH  2400
 H0630-541   2A0626-541   1.98  .18   2.23  .13   SC0630-541   6  *  .0502 V   2.520
5.55   6.25   4U0627-54
                               ----------------------------------------------------
--------------------------------------------------------- H0906-095   2A0906-095   3.96
 .28   4.16  .26   ABELL 754   6  *  .0537 C1   2.440   12.3   12.9   4U0900-09

      ---------------------------------------------------------------------------------
-------------------------- H0917-074   1.36  .28   1.21  .3   7
    2.500                                  ----------------------------------
------------------------------------------------------------- H0943-141   2A0943-140
 3.14  .25   3.97  .54   NGC2992   2  *  .0062 DV   2.175   .114   .143   4U0937-
12
          ---------------------------------------------------------------------------
----------------------------- H0952+699   2A0954+700   1.32  .2   1.17  .2   M82
   2  *  .0013 DV   2.480   .0024   .0021   1M0943+712
                                                          4U0954+70
                                                                                 ---
-------------------------------------------------------------------------------------------------------
---------------- H1019+203   A1021+198   1.71  .24   .96  .3   NGC3227   2  *  .003
3 W1   2.175   .0175   .0098   -------------------------------------------------------
------------------------------------------------------- H1034-273   2A1033-270   2.19  .2
1   2.25  .3   ABELL 1060  6  *  .0114 M   2.880   .355   .365   4U1033-26

  ---------------------------------------------------------------------------------------------
----------------------

 TAPE NO.  1            FILE NO.  1
 RECORD  5              LENGTH  2400
 H1136-375   2A1135-373   1.95  .23   <.6   NGC3783   1  *  .0091 W1   2.175
 .152   4U1136-37
                              ------------------------------------------------------
--------------------------------------------------------- H1208+397   2A1207+397   6.34
 .26   10.64  .36   NGC4151   1  *  .0033 W1   2.070   .0607   .104   1M1207+397

    4U1206+39
                     --------------------------------------------------------------------
------------------------------------------------- H1219+305   2A1219+305   1.61  .25   1.3
 .3   1219+305   3  *   2.340                    -------------------------------
-------------------------------------------------------------------------------- H1226+0
23   2A1225+022   3.46  .26   3.8  .37   3C273   5  *  .158  MS   2.040   81.6
```

```
89.6        4U1226+02
                                                       H1228+127      2A1228+125     14.2     .33
14.25  .33   VIRGO CL.   6   *   .0037 DV    2.850         .239            .240       1M1228+127
                                                                                              4
U1228+12
                                          H1238-049     4U1240-05       1.71  .26       1.09  .41   NG
C4593      1   *   .0085 DV    2.175         .116          .0741
                                                                              H1246-410       2A
1246-410       5.15  .23       5.64  .37.  CEN CL.     6   *   .0118 FO    2.740        .851        .932
  1M1247-410

 TAPE NO.    1                 FILE NO.    1
 RECORD   10                   LENGTH   2400
                     H2158-321       2A2151-316      2.00  .23       1.4   .29   NGC7172      4  **  .
009  DV   2.570          .180          .126
                                                               H2209-471                1.07  .21
1.83  .28   NGC7213       1   *   .0058 DV    2.175         .0338         .0578
       H2216-027      2A2220-022       1.55  .24        .98  .29   3C445       2   **   .0562 OKP   2.175
     4.71          2.98
                                                  H2233-261        2A2237-256       1.39  .22        1.94
 .3    NGC7314       2  **   .0056 DV   2.175          .0410         .0572
                                                                                        H2301+0
86     2A2259+085       1.77  .25       1.45  .39   NGC7469       1   *   .0167 W1    2.175        .466
    .382        4U2300+08
                                                        H2302-090       2A2302-088        1.88  .25
 2.3    .34   MCG2-58-22   1   *   .0479 W2    2.175        4.14          5.06        4U2305-07

                  H2316-426       2A2315-428       2.51  .23        3.04  .29   NGC7582       2   *   .004
8 DV    2.175          .0543          .0658
                                                              H2342+089        4U2344+08        1.31  .2
7         .93  .33    ABELL2657    6   *   .0414 N     2.520        2.49         1.77

 TAPE NO.    1                 FILE NO.    1
 RECORD    11                  LENGTH   2400
                        COLUMN CAPTIONS:
                                                                  (1) : H NAME
          (2) : PREVIOUS NAMES
                                                     (3) : 1ST SCAN FLUX AND 1-SIGMA ERROR (R15 COUNTS/
SEC)
                                                                                          (4) : 2N
D SCAN FLUX AND 1-SIGMA ERROR (R15 COUNTS/SEC)
                                       (5) : IDENTIFICATION
                                                                              (6) : TYPE OF OBJECT: 1
 = SEYFERT 1 GALAXY
                         2 = SEYFERT 2, NELG, N OR OTHER ACTIVE GALAXY
                                            3 = BL LACERTE OBJECT
                                                              4 = NORMAL GALAXY
                                                                                5 = QSO
```

6 = CLUSTER OF GALAXIES
7 = UNIDENTIFIED

TAPE NO. 1 FILE NO. 1
RECORD 12 LENGTH 2400

(7) : QUALITY OF IDENTIFICATION: * = CERTAIN: SAS-3 OR HEAO-1 MODULATION COL
LIMATOR POSITION OR EINSTEIN OBSERVATORY P ** = POSSIBLE

(8) : REDSHIFT
VALUE AND REFERENCE:
B = BAHCALL,N.A.,SARGENT,W.L.W.,1977,AP.J.,217,L19
B2 = BAHCALL,N.A.,AP.J.,217,L77
C1 = CORWIN,H.G.JR.,1971,PUBL.ASTRON.SOC.PA
CIFIC,83,320
C2 = CORWIN,H.G.JR.,19
74,A.J.,79,1356
CM
R = CANIZARES,C.R.,MCCLINTOCK,J.E.,RICKER,G.R.,1978,AP.J.,226,L1
CTB = CHARLES,P.,THORSTENSEN,J.,BOWYER,S.,1979,NATURE,281,285
DV =DEVAUCOULEURS,DEVAUCOULEURS AND CORWIN SECOND REFERENC
E CATALOG OF BRIGHT GALAXIES 1976
F = FABER,S.,DRESSLER,A.,1977,A.J.,8
2,167
FD = FOSBURY,R.A
.E.,DISNEY,M.J.,1976,AP.J.,207,L75
FO = FORMAN,W.,JONES,C.,TANANBAUM,H.,1976,AP.J.,206,L29
H = HINTZEN,P.,SCOTT,J.S.,1979,AP.J.,232,L145
HSM = HINTZEN,P.SCOTT,J.S.,MCKEE,J.D. 1980 AP.J. IN P
RESS
L = LUGGER,P.,1978,AP.J,221,74
5
M = MELNI
CK,J.,SARGENT,W.,1977,AP.J.,215,401
MA = MACCAGNI,D.,TARENGHI,M.,COOKE,B.A.,MACCACARO,T.,PYE,J.P.,RICKETTS,M.J.,CHINCARINI,G
.,1978,ASTRON.&ASTROPHYS

TAPE NO. 1 FILE NO. 1
RECORD 13 LENGTH 2400
MQ = MELNICK,J.,QUINTANA,H.,1975,AP.J.,198,L97
MP = MCHARDY,J. AND PYE,J IAU CIRCULAR 3587 1981
MS = SCHMIDT,M.,1968,AP.J.,151,393
N = NOONAN,T.,1973,A.J.,78,
26
OKP = OS
TERBRCK,D.E.,KOSKI,A.T.,PHILLIPS,M.M.,1976,AP.J.,206,898
S = SPINRAD,H.,1977,PUB.A.S.P.,89,116
SC = SCHWARTZ,D.,SCHWARZ,J,TUCKER,W.,,1980,AP.JLETT. 238,L59
V = VIDAL,N.V.,1975,PUBL.ASTRON.SOC.PACIFI
C,87,625
W1 = WEEDMAN,D.W.,1977
,ANN.REV.ASTRON.ASTROPHYS.,15,69
W2
= WEEDMAN,D.W.,1978,MON.NOT.R.ASTR.SOC.,184,11P
W3 = WEEDMAN,D.W.,1979,PROC.IAU GENERAL ASSEMBLY,MONTREAL
WF = WEST,R.M.,FRANDSEN,S.,1980,ESO SCIENT. PREPRINT N.110
,

(9) : CONVERSION FACTOR
(1.E-11 ERGS/CM2 SEC PER R15 COUNTS/SEC)

(10) : 1ST SCAN LUMINOSITY (1.E44 ERGS/SEC)

(11) : 2ND SCAN LUMINOSITY (1.E44 ERGS/
SEC)

(12) : NOTES

TAPE NO. 1 FILE NO. 1
RECORD 14 LENGTH 360
1.IPC DETECTION BUT NOT IDENTIFIED AT PRESENT
2.MULTIPLE CLUSTER FORMAN ET AL 1981
3.MULTIPLE CLUSTERS PERRENOD AND HENRY 1981